INTERNATIONAL ATOMIC ENERGY AGENCY
UNITED NATIONS EDUCATIONAL, SCIENTIFIC AND CULTURAL ORGANIZATION
INTERNATIONAL CENTRE FOR THEORETICAL PHYSICS
I.C.T.P., P.O. BOX 586, 34100 TRIESTE, ITALY, CABLE: CENTRATOM TRIESTE

UNITED NATIONS INDUSTRIAL DEVELOPMENT ORGANIZATION

INTERNATIONAL CENTRE FOR SCIENCE AND HIGH TECHNOLOGY
c/o INTERNATIONAL CENTRE FOR THEORETICAL PHYSICS 34100 TRIESTE (ITALY) VIA GRIGNANO, 9 (ADRIATICO PALACE) P.O. BOX 586 TELEPHONE 040-224572 TELEFAX 040-224575 TELEX 460449 APH I

SMR. 628 - 23

Research Workshop in Condensed Matter, Atomic and Molecular Physics (22 June - 11 September 1992)

Working Party on: "Energy Transfer in Interactions with Surfaces and Adsorbates" (31 August - 11 September 1992)

"Valence Loss Spectra in Stem." (Scanning Transmission Electron Microscope)

P.M. ECHENIQUE
Universidad del Paris Vasco
Dep. de Fisica de Materiales
Aparttado 1072
San Sebastian 2080
SPAIN

These are preliminary lecture notes, intended only for distribution to participants.

VALENCE LOSS SPECTRA IN STEM. (Scanning Transmission Electron Microscope)

A. Rivacoba
M.E. Uranga
P.M. Echenique

Euskal Herriko Unibertsitatea.- Euskadi.- Spain

A. Howie - Cambridge
P.H. Ritchie - ORNL
F. Flores - Madrid
J.B. Pendry. - Imperial

SPATIALLY LOCALIZED SPECTROSCOPY IN STEM

Main point (unique to STEM).

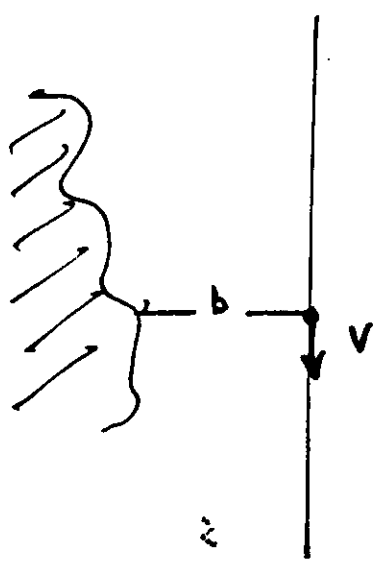

The development of Scanning Transmission Electron Microscope (STEM) has stimulated and renewed the interest in the interaction of high energy electron beams with surfaces and small particles.

In a typical STEM configuration a well-focused 0.5nm probe of 100keV provides a high-resolution transmission scanning image for samples with complex structures, such as catalyst or semiconductor devices. It also yields from selected regions of the target, energy loss spectra (EELS), with a resolution .of about 1 eV.

Some **examples** in which the spectra contain details relating to significant microstructural features which can not be resolved by the standard STEM imaging techniques.

Walls and Howie. Suggested the presence of a 1nm layer of SiO at the Si-SiO_2 interfase on the basis of an analysis of the observed intensity of the 8eV interfase plasmon. [Ultramicroscopy, **28**,40(1989)]

Ugarte, Colliex and Trebbia: Ascribe the presence of an unexpected peak at 3 - 4 eV localised at the external surface of Si spheres with an oxide coating , to a 0.5nm thick layer of amorfous Si, formed after reduction of the external oxide surface. Phys. Rev B**45**, 4332 (1992)

Ugarte
Phys. Rev. B15

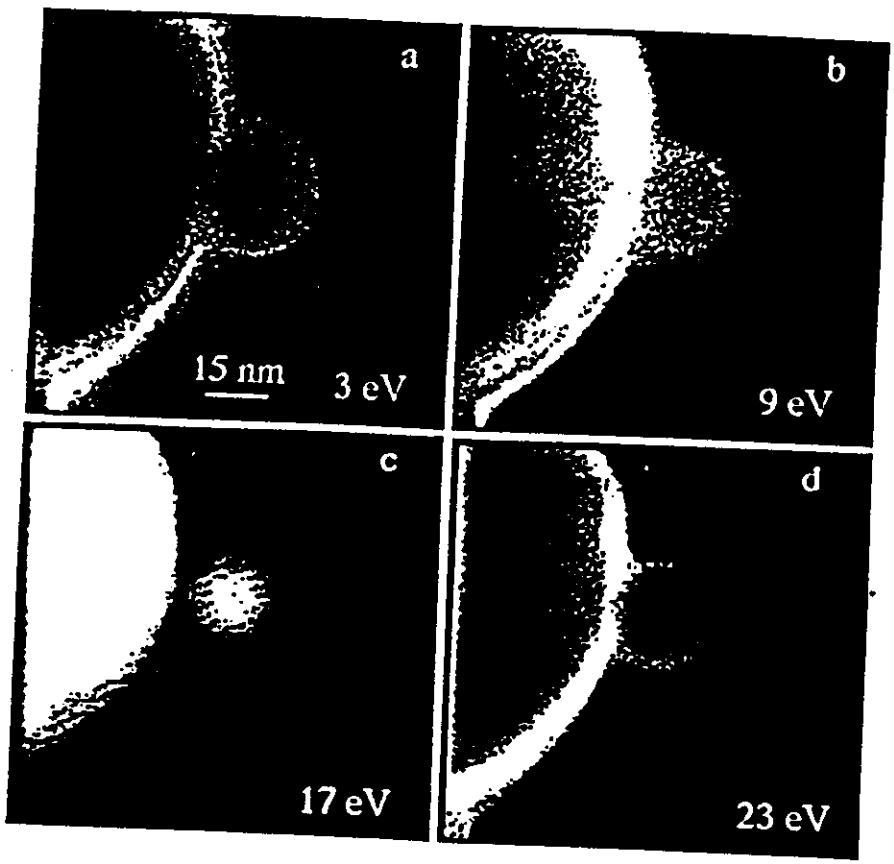

Ugarte, Colliex and Trebbia, Phys. Rev B45 4332 (1992)

Figure 3

VALENCE LOSS SPECTRA IN STEM (Scanning Transmission Electron Microscope)

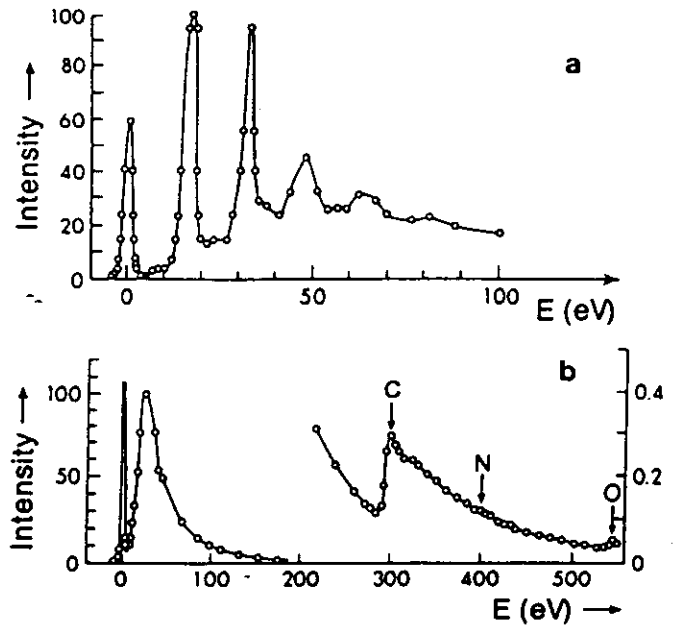

Figure 1.7. (a) Energy-loss spectrum of 5.3-keV electrons transmitted through a thin foil of aluminum (Ruthemann, 1941), exhibiting plasmon peaks at multiples of 16 eV loss. (b) Energy-loss spectrum of 7.5-keV electrons transmitted through a thin film of collodion, showing *K*-ionization edges arising from carbon, nitrogen, and oxygen (Ruthemann, 1942).

Atomic inner shell excitations ($\Delta E \sim 10^2 eV$)

The characteristic loss features associated with atomic inner shell exciations provide rather direct chemical analysis on an atomic scale and via the study of their detailled shape some information about local bonding and electronic structure.

Valence electron excitations ($\Delta E \leq 50$ eV)

The loss in this region is much more intense, but has not been so frequently used because the interpretation of the data is much more complex.

The classical dielectric theory is enough: *"A new lease of life for Fermi's theory"*. (A. Howie)

Bulk $\Rightarrow$ Fermi $\Rightarrow \propto \mathbf{Im}\left[\frac{-1}{\varepsilon(\omega)}\right]$

Surfaces

Plane and film $\Rightarrow$ Ritchie (1957) $\Rightarrow \propto \mathbf{Im}\left[\frac{1}{\varepsilon_a+\varepsilon_b}\right]$

Sphere (dipole) $\Rightarrow$ Fujimoto & Komaki (1968) $\Rightarrow \propto \mathbf{Im}\left[\frac{3}{\varepsilon_a+2\varepsilon_b}\right]$

To study

Interfaces
Small particles
Inhomogeneous specimens

LOCALIZATION IN INELASTIC SCATTERING

The basic mechanism in the inelastic scattering is not a contact interaction but the Coulomb potential → the spatial localization of the inelastic scattering is not necesarily determined by the size of the incident probe.

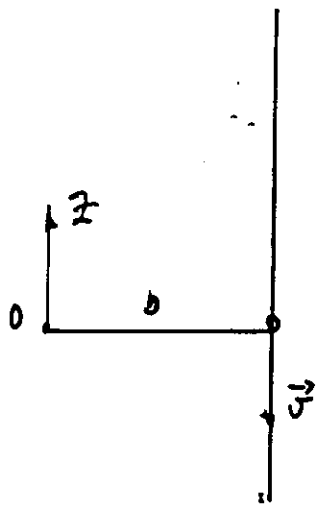

The localization of this process can be visualized by analysing the Fourier components of the electric field $\mathbf{E}(\omega)$ induced at the point **o** by the moving charge when moving in a medium

$$E_z = \frac{-i\omega}{v^2}\left[\frac{1}{\varepsilon(\omega)} - 1\right]\left[\frac{2}{\pi}\right]^{1/2} K_0\left[\frac{\omega b}{v}\right] \rightarrow \propto e^{-\frac{\omega b}{v}} \qquad b > v\omega^{-1}$$

$$E_\perp = \frac{\omega}{v^2}\left[\frac{2}{\pi}\right]^{1/2} \frac{1}{\varepsilon(\omega)}\, K_1\left[\frac{\omega b}{v}\right] \rightarrow \propto e^{-\frac{\omega b}{v}} \qquad b > v\omega^{-1}$$

Thus the Coulomb interaction is negligible for values of the impact parameter larger than $v\omega^{-1}$.

The former idea can be stated by a <u>simple time of flight argument.</u>

Duration of the electric pulse bv^{-1} → Thus ω up to vb^{-1}.

$$b \approx \frac{v}{\omega}$$

The same result can be obtained from kinematic arguments.

$$q^2 = \left[\frac{\omega}{v}\right]^2 + q^2\vartheta^2 \qquad \vartheta \text{ deflection angle}$$

thus when there is not deflection

$$\frac{\omega}{v} \sim q(0) \sim b^{-1}$$

This is really a consequence of the uncertainty principle: the larger the momentum transfer is, the more highly localised is the interaction.

EXCITATION OF ELECTRONIC TRANSITIONS BY A COHERENT e^- IRRADIATION.

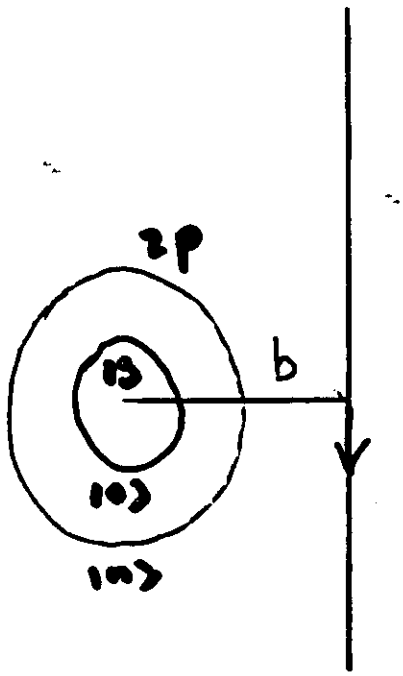

Probability of the transition $|0\rangle \rightarrow |n\rangle$ induced in the target by a broad e^- beam in the direction of the z axis.
Time-dependent perturbation theory (a.u.)

$$\sigma_{n0} = \frac{4}{v}\int \frac{dq}{q^4} \left| \rho_{n0}(q) \right|^2 \delta(\mathbf{v}.\mathbf{q} - \frac{q^2}{2} - \omega_{n0})$$

where $\mathbf{q} = \mathbf{k}_0 - \mathbf{k}_f$

$\omega_{n0} = \omega_n - \omega_0$

$$\rho_{n0}(\mathbf{q}) = \langle n | e^{iqr} | 0 \rangle$$

Neglecting the recoil, and introducing the impact parameter **b** as the variable conjugate to the perpendicular component of the momentun transfer **Q**; $\mathbf{q}=(\mathbf{Q},q_z)$

$$\sigma_{n0} = \int d\mathbf{b} \left| a_{n0}(\mathbf{b}) \right|^2$$

where

$$a_{n0}(\mathbf{b}) = \frac{1}{\pi v}\int \frac{d\mathbf{Q}\ e^{i\mathbf{Q}\mathbf{b}}}{Q^2 + \left(\frac{\omega_{n0}}{v}\right)^2} \rho_{n0}(Q, \frac{\omega_{n0}}{v}) + O(v^{-2})$$

This expression is (up to the terms involving v^{-2}) identical to that obtained for a classical point electron traveling with constant velocity v at impact parameter **b** .(First obtained for protons by Frame(1931) and Mott(1931).

Quantal corrections are small for STEM electrons ($v \sim 10^2$ a.u.).

The spatial extension of the contributing part of the beam $\sim v\omega^{-1}$

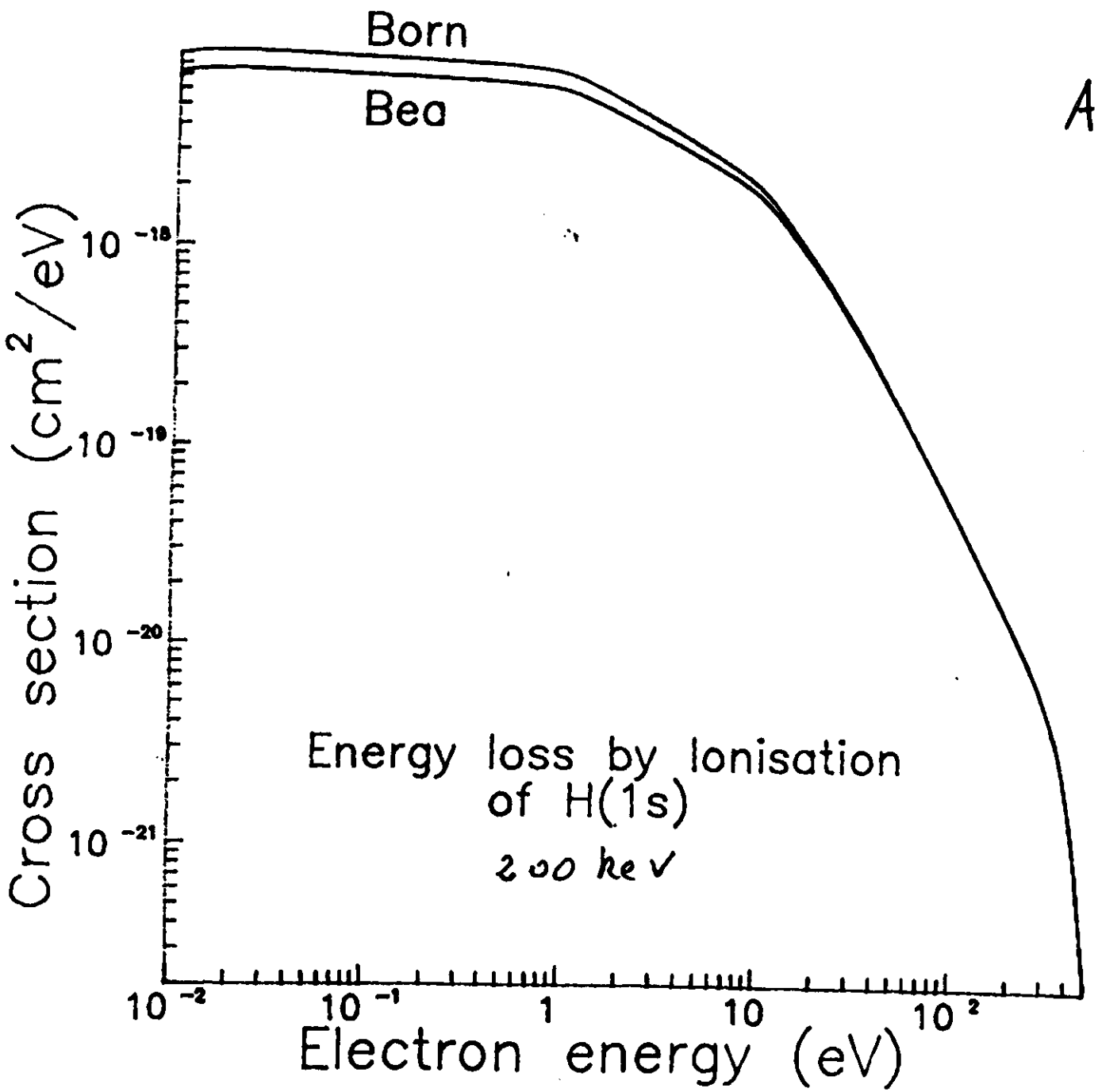
Born
Bea
A Salim.
Cross section (cm^2/eV)
10^{-18}
10^{-19}
10^{-20}
10^{-21}
Energy loss by Ionisation
of H(1s)
200 keV
10^{-2}
10^{-1}
1
10
10^{2}
Electron energy (eV)

Quantal corrections to the scattering probability of fast electrons by a hidrogen atom.

(R.H. Ritchie, Phil. Mag. A44,931 (1981))

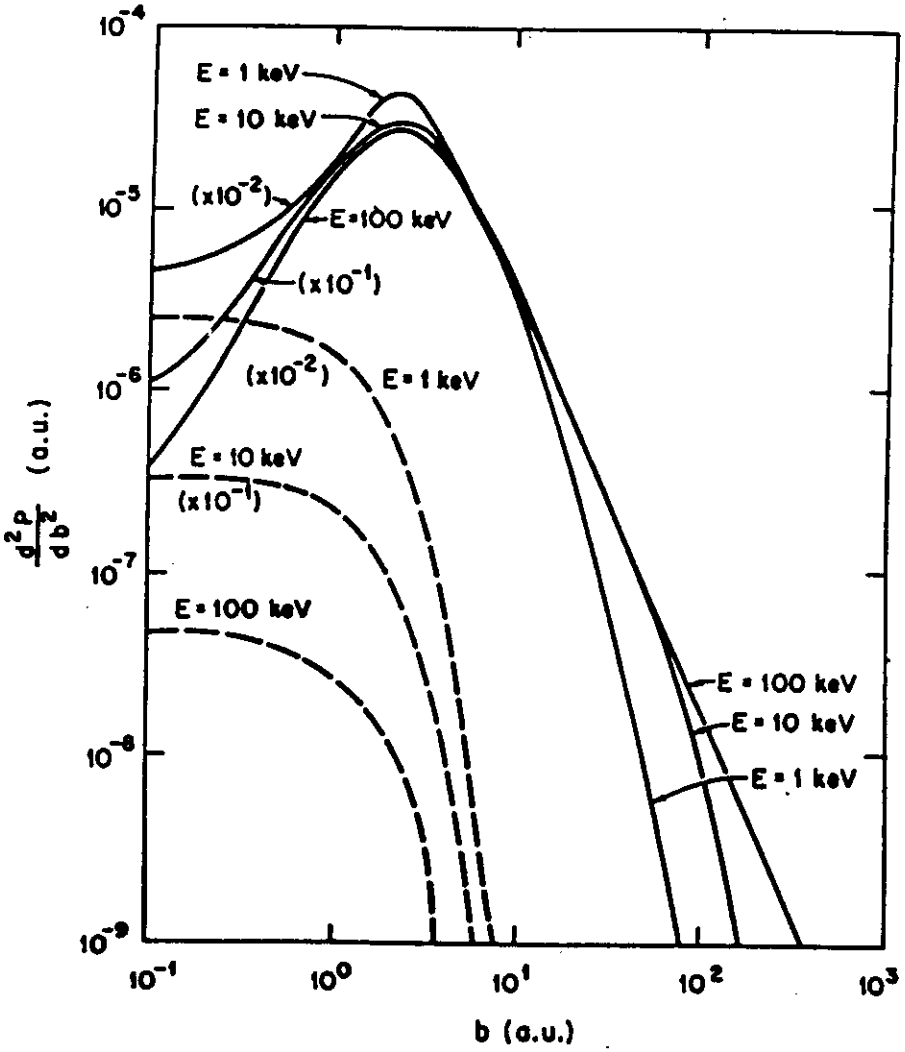

differential probability of excitation of a hydrogen atom by fast electrons with various energies E as a function of impact parameter b. The results, calculated as if the electron were a point classical particle, are shown as solid lines, and the quantal corrections are shown as dashed lines. The latter are all negative but are shown in magnitude only. The hydrogen atom is assumed to be excited from the ground state to the 2p states. To render the results easily visible, the distributions corresponding to $E = 1$ keV have been scaled down by a factor of 100, while those corresponding to 10 keV have been scaled down by a factor of 10.

Quantal corrections to the scattering probability of fast electrons by a sphere (dipolar mode).

(R.H. Ritchie, Phil. Mag. A44,931 (1981))

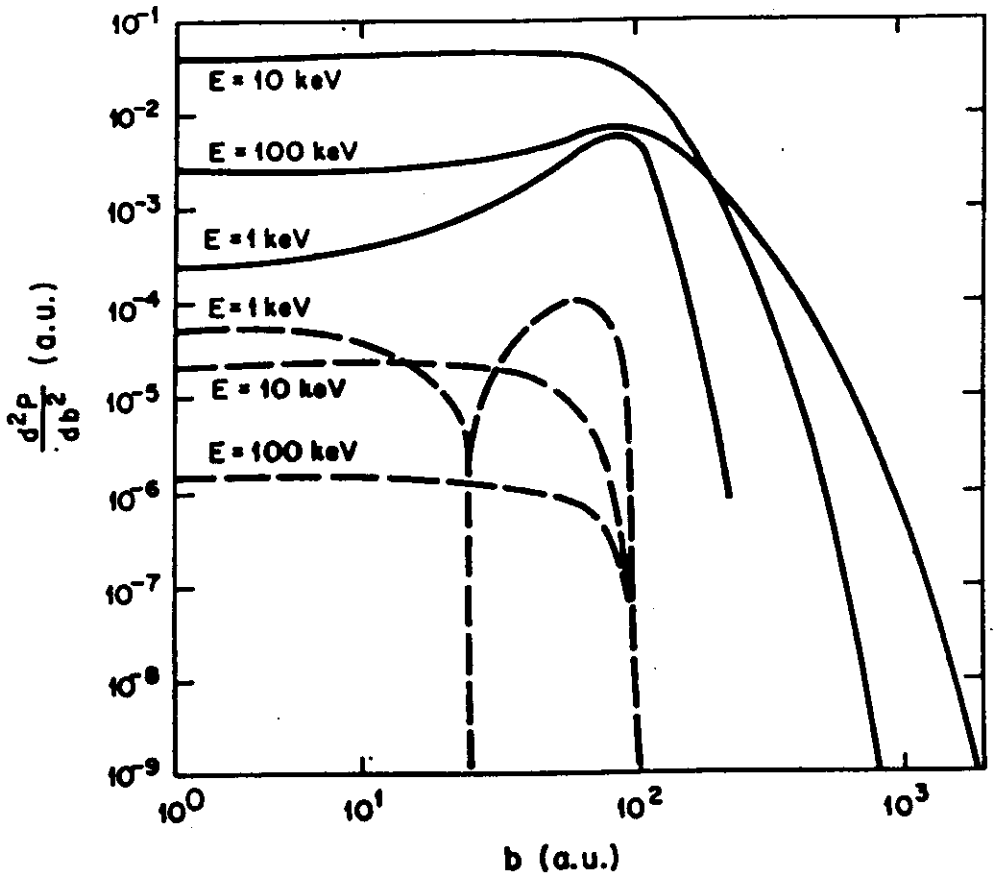

differential probability of excitation by fast electrons of the spherical dipole surface plasmon on an aluminium sphere with a radius of 50 Å. The distributions are plotted as a function of impact parameter b for electron kinetic energies of 1, 10 and 100 keV. The solid curves depict the classical results, while the dashed curves show the quantal corrections. The quantal correction at 1 keV for values of b lying in the interval $30 \leqslant b \leqslant 95$ a.u. is actually negative but has been plotted as shown for convenience.

EXCITATION OF ELECTRON TRANSITIONS by a MICRO PROBE ELECTRON.

RITCHIE & HOWIE. (1st Born).

initial state $\psi_i(\underset{\sim}{r}) = \phi(\underset{\sim}{r} - \underset{\sim}{b}) \cdot$ ('plane wave' $\underset{\sim}{z}$-direction)

Final state Plane wave

$$P_n(\underset{\sim}{b}) = \int d^2\underset{\sim}{\rho} \, |\phi(\underset{\sim}{\rho} - \underset{\sim}{b})|^2 \cdot P_n^{\text{classical}}(\underset{\sim}{\rho})$$

$P_n^{\text{quantum}}(\underset{\sim}{b})$

Prob. of finding the electron at $\underset{\sim}{\rho} - \underset{\sim}{b}$ in microprobe.

Classical

Prob. of exciting n^{th} state by a point electron at impact p. $\underset{\sim}{b}$

PLANAR INTERFACES

Many cases

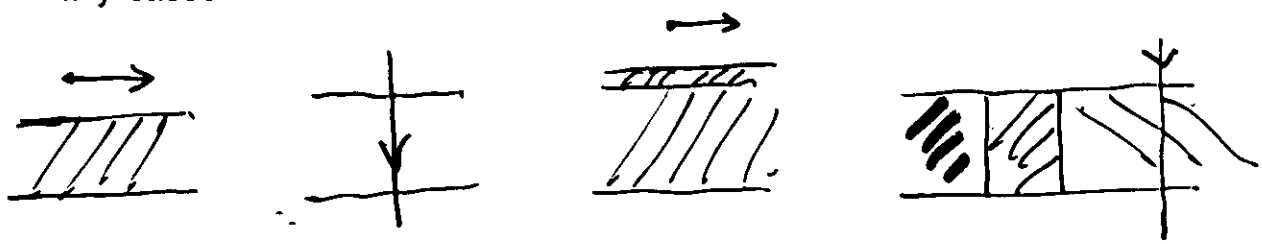

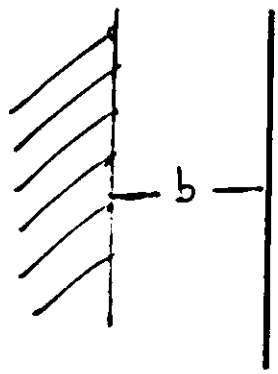

Charge moving parallelly to the interfase.
External beam

$$\frac{dW}{dz} = \frac{2}{\pi v^2}\int_0^{\infty} K_0\left(\frac{\omega b}{v}\right)\,\omega\,\mathrm{Im}\left[\frac{\varepsilon(\omega)-1}{\varepsilon(\omega)+1}\right]d\omega$$

P.M.E and J. Pendry J. Phys. C8 2936 (1975)

$$K_0\left(\frac{\omega b}{v}\right) = \int_0^{\infty} dq \frac{e^{-2b\sqrt{q^2+(\omega/v)^2}}}{\sqrt{q^2+\left[\frac{\omega}{v}\right]^2}}$$

Free electron case: Imaginary part of the self-energy:

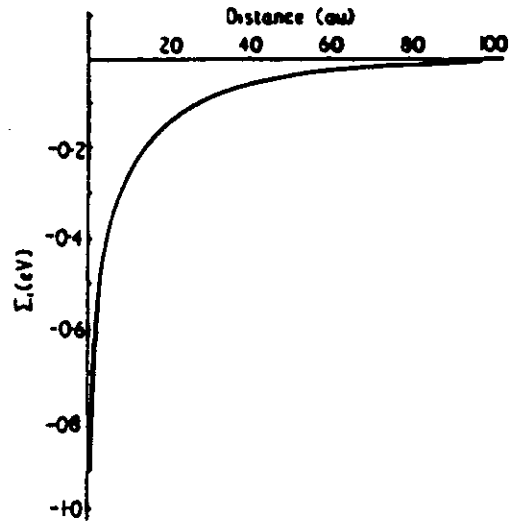

$$\Sigma_i(b) = \frac{-\omega_s}{2}\,K_0\left[\frac{2\omega_s b}{v}\right] \quad ; \quad \omega_s = \frac{\omega_p}{\sqrt{2}}$$

$$K_0(x) = \begin{cases} -\ln\left(\frac{x}{2}\right) & x<<1 \\ \sqrt{\frac{\pi}{2x}}\,e^{-x} & x>>1 \end{cases}$$

Figure 1. Variation of the imaginary part of the self-energy (eV) with the distance (au) to the surface for parallel incidence: $\omega_s = 15/\sqrt{2}$ eV. $E = 40$ keV.

The divergence at the surface is due to the fact that at such a small distances large momentum transfer is involved → the q-dependence of the response function can not be neglected.

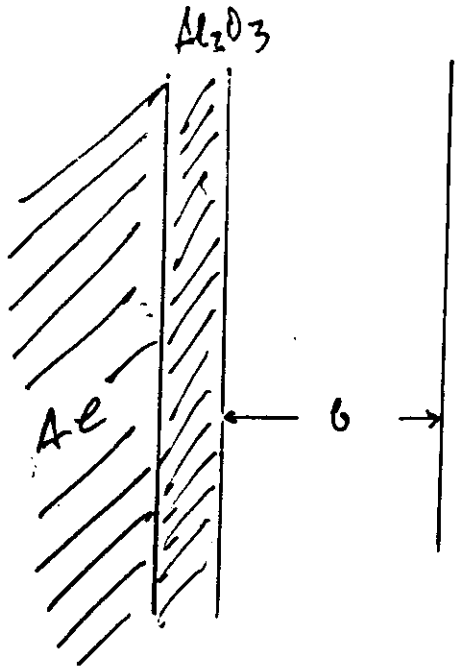

P. E. Batson
Ultramicroscopy 11, 299 (1983).

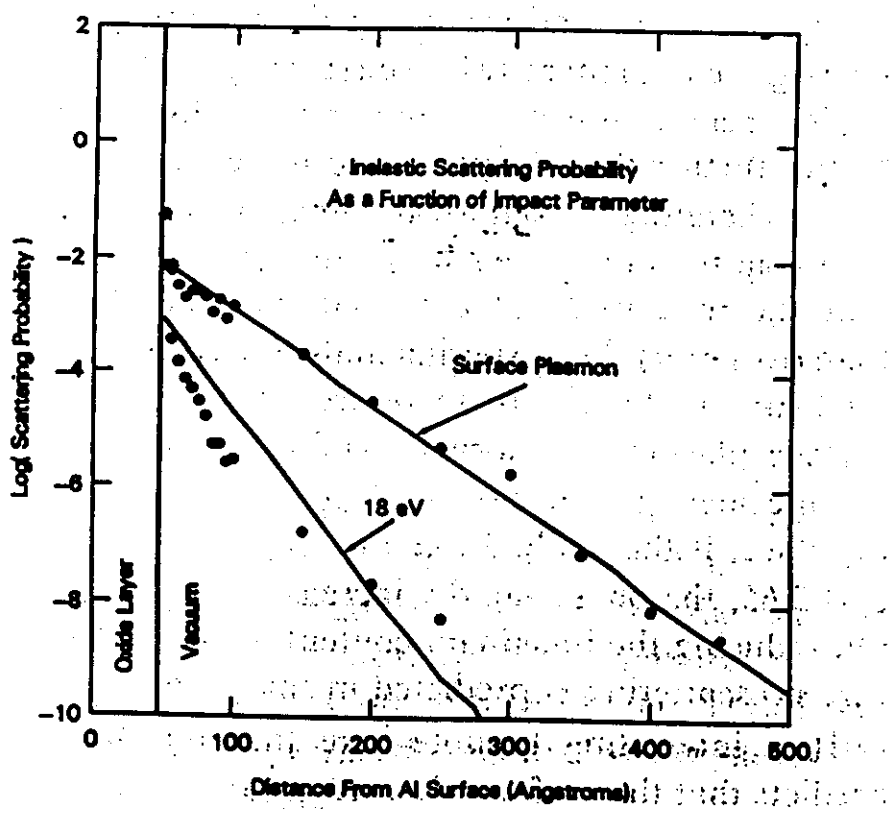

Fig. 4. Scattering intensity as a function of impact parameter for two energies compared to the model results.

Q Inside

$z < c$ $\quad P(\omega) = \frac{2}{\pi v^2}\left\{ Im\left(\frac{-1}{\varepsilon(\omega)}\right) \ln\left(\frac{q_c v}{\omega}\right) \right.$

$+ \left[Im\left(\frac{-2}{\varepsilon+1}\right) - Im\left(\frac{-1}{\varepsilon}\right) \right]$

$\left. \times K_0\left(\frac{2\omega z}{v}\right) \right\}$

- Begrenzung ↓ Ritchie ——— C. Monreal (SPLEES).
- Non locality ; Complicated geom.
- Retardation. Garcia Molina et al.

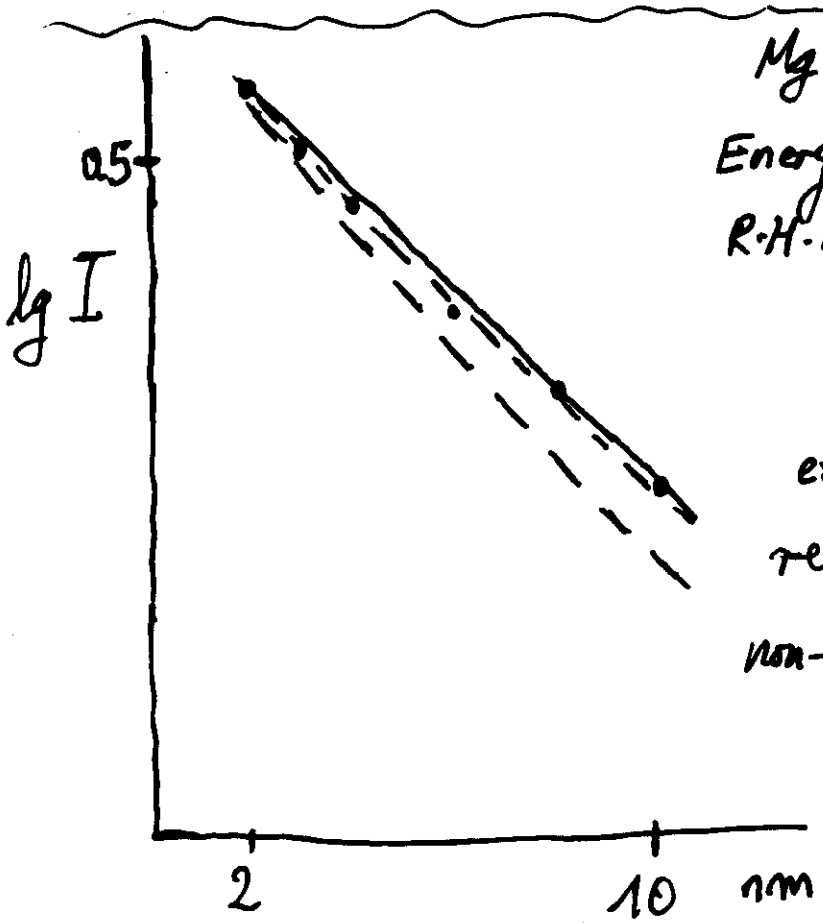

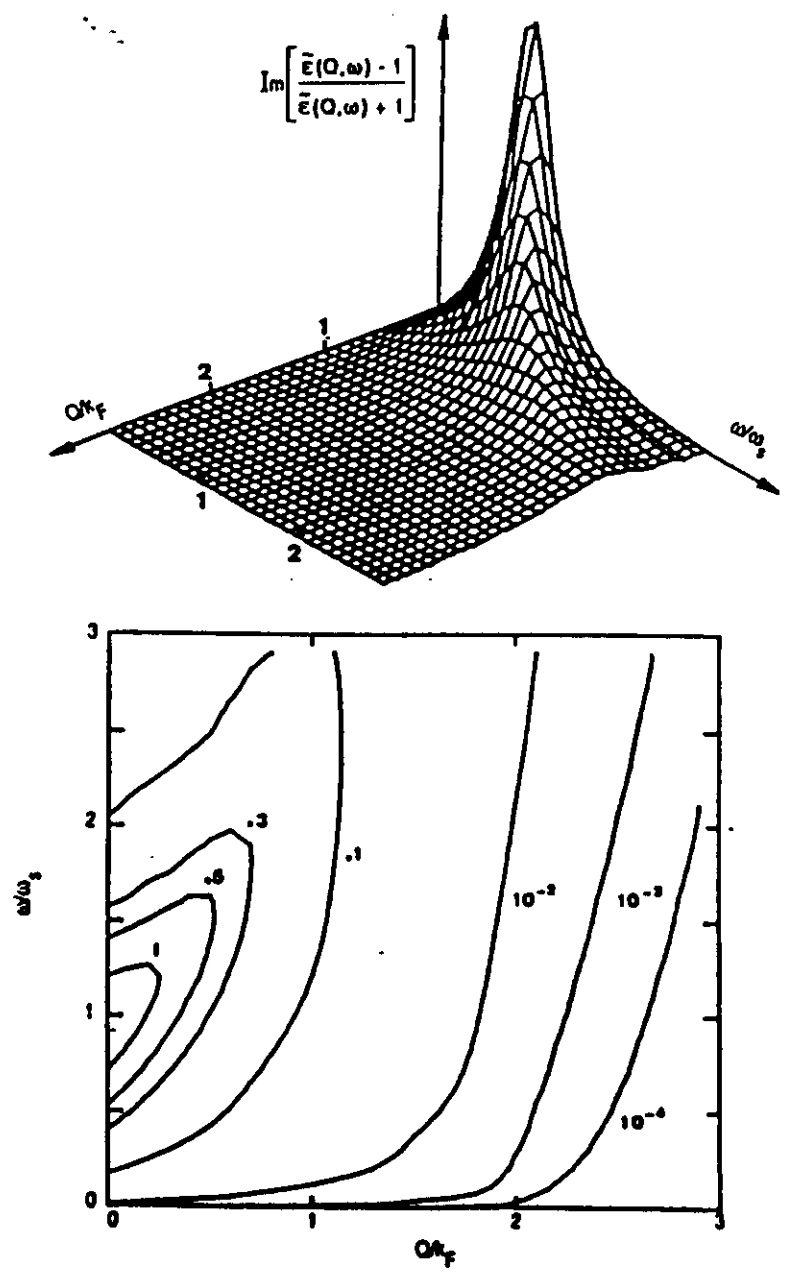

Fig. 2. Surface energy-loss function calculated using the Mermin dielectric function $\epsilon(k, \omega)$ given by expression (21), with $r_s = 1.75$ and damping constant $\gamma = 8$ eV as a function of energy (in units of the surface plasmon energy, ω_s) and momentum Q in units of the Fermi momentum k_F: (a) contour plots; (b) three-dimensional plot.

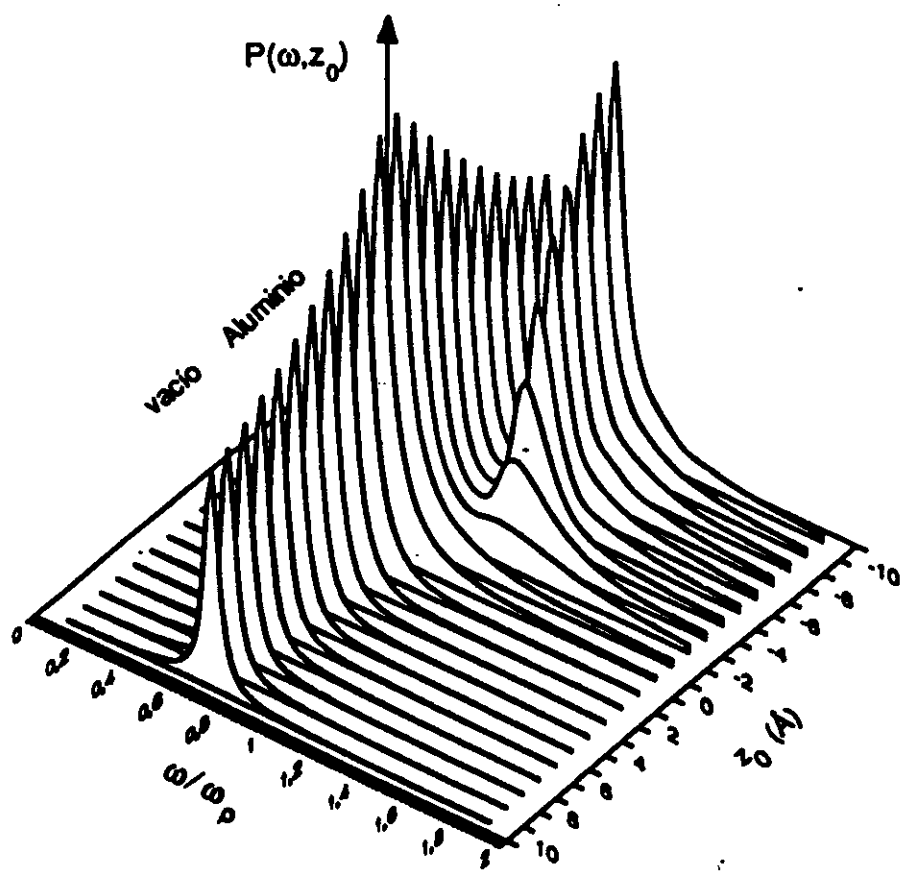

Figura III.5: Espectros de pérdida de energía calculados con las expresiones no locales, para distintos valores del parámetro de impacto, en un intervalo de 10 Å a través de una interfase Al-vacío. La energía del electrón incidente es de 100 KeV. Los valores negativos del parámetro de impacto z_0 corresponden a trayectorias en el metal y los positivos a trayectorias en el vacío.

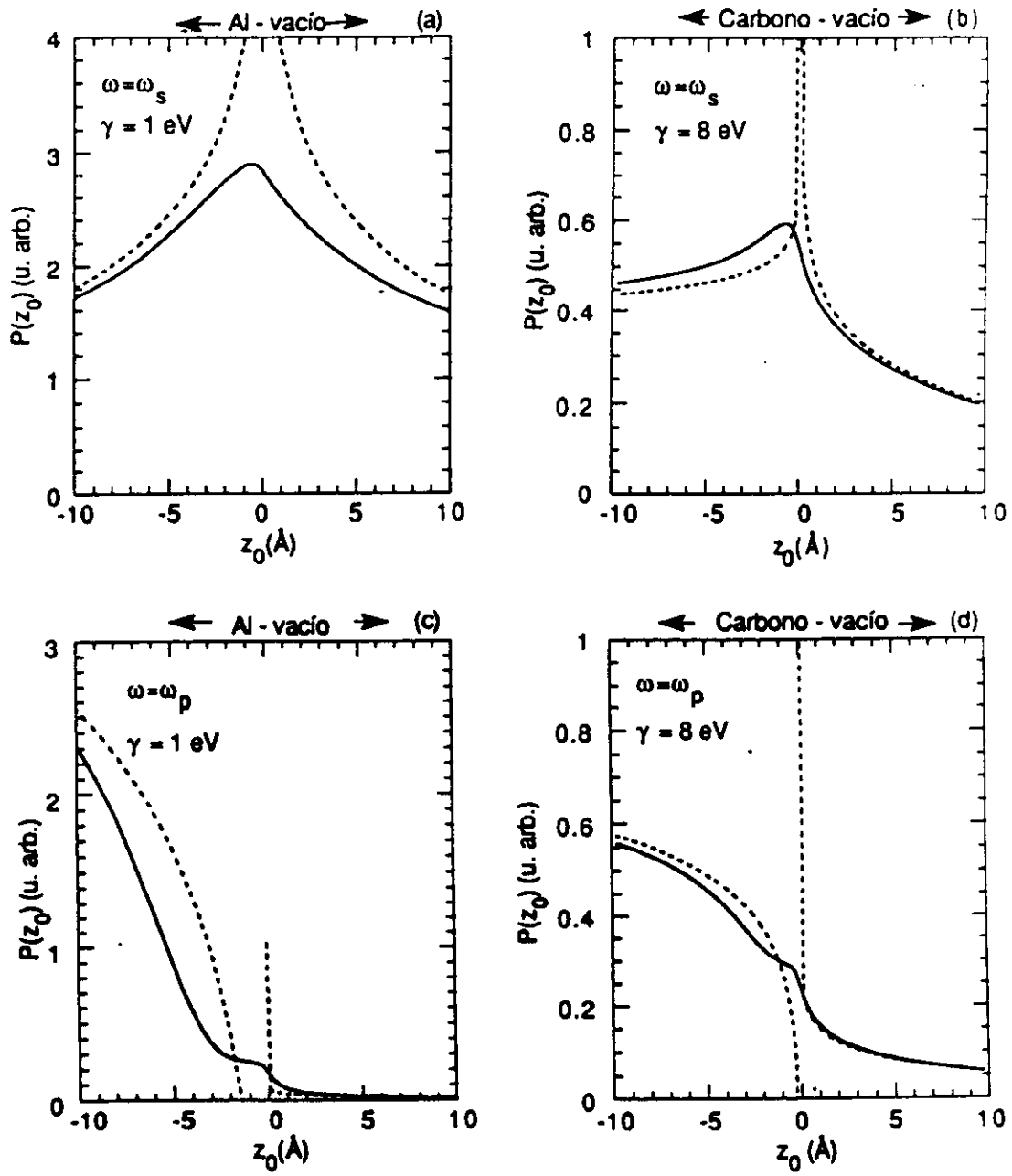

Figura III.7: Probabilidad de excitación en función del parámetro de impacto para la energía del plasmón de volumen (c) , (d) y de superficie (a), (b). La energía del electrón del haz es de 100 KeV. La probabilidad local se ha representado con línea a trazos y la no local con línea continua. Para $z_0 < 0$ el electrón viaja en el Al ($r_s = 2.07$, $\gamma = 1$ eV) (figuras (a) y (c)) o en C ($r_s = 1.75$, $\gamma = 8$ eV) (figuras (b) y (d)) y para $z_0 > 0$ en el vacío.

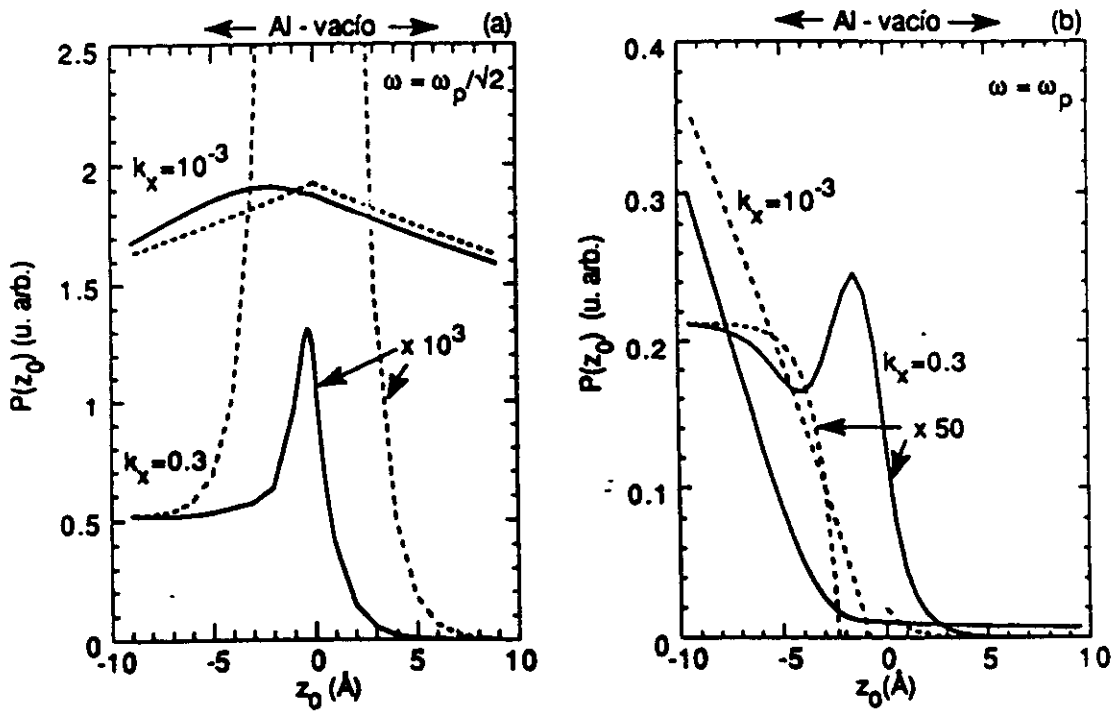

Figura III.4: Probabilidad $P(k_x,\omega)$ de excitación de plasmones de (a) superficie de energía $\omega_s = \omega_p/\sqrt{2}$ y (b) de volumen de energía ω_p y de transferir momento k_x al medio, en función del parámetro de impacto del electrón, a través de una interfase vacío-metal. El metal es aluminio ($r_s = 2.07$ y amortiguamiento $\gamma = 1eV$) y la energía del electrón incidente 100 KeV.

SPHERICAL PARTICLE

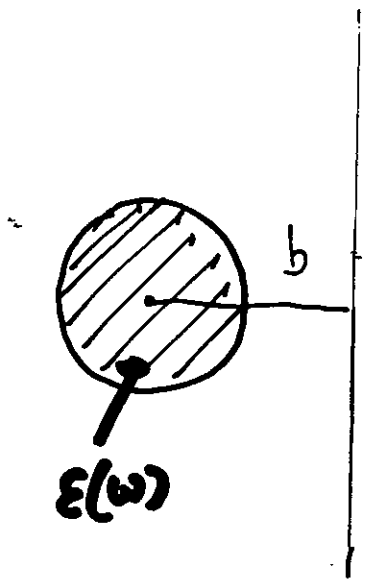

Dipolar aproximation $b >> a$

$E(z)$ ~ constant over the sphere

$$J(\omega) = -i\,\omega P(\omega)$$

The energy loss W

$$W = \int dt \int_{sph.} dr\ J.E. = \int_0^{\infty} \omega\, d\omega\, P(\omega)$$

$P(\omega)$ is the probability of lossing the energy ω.

$$P_\omega(b) = \frac{a^3}{\pi} Im\left[\frac{\varepsilon(\omega)-1}{\varepsilon(\omega)+2}\right] |E(\omega)|^2$$

In the non-retarded limit

$$P(\omega) = \frac{4a}{\pi v^2} Im\left[\frac{\varepsilon(\omega)-1}{\varepsilon(\omega)+2}\right]\left(\frac{\omega a}{v}\right)^2\left[K_o^2\left(\frac{\omega b}{v}\right) + K_1^2\left(\frac{\omega b}{v}\right)\right]$$

This expression is properly the first term of the following series,valid for any value of b >a

$$P_\omega(b) = \frac{4a}{\pi v^2} \sum_{l=0}^{\infty} \sum_{m=0}^{l} \frac{2-\delta_{m0}}{(l-m)!(l+m)!}\ Im\left[\frac{l(\varepsilon(\omega)-1)}{l\varepsilon(\omega)+l+1}\right]\left(\frac{\omega a}{v}\right)^{2l} K_m^2\left(\frac{\omega b}{v}\right)$$

where the contribution of all the multipolar terms has been taken into account (Ferrel and P.M.E, (1985))

Here the dependence on the impact parameter is given by

$$K_m^2\left(\frac{\omega b}{v}\right) \propto e^{-\frac{2\omega b}{v}} \qquad b \geq 2v\omega^{-1}$$

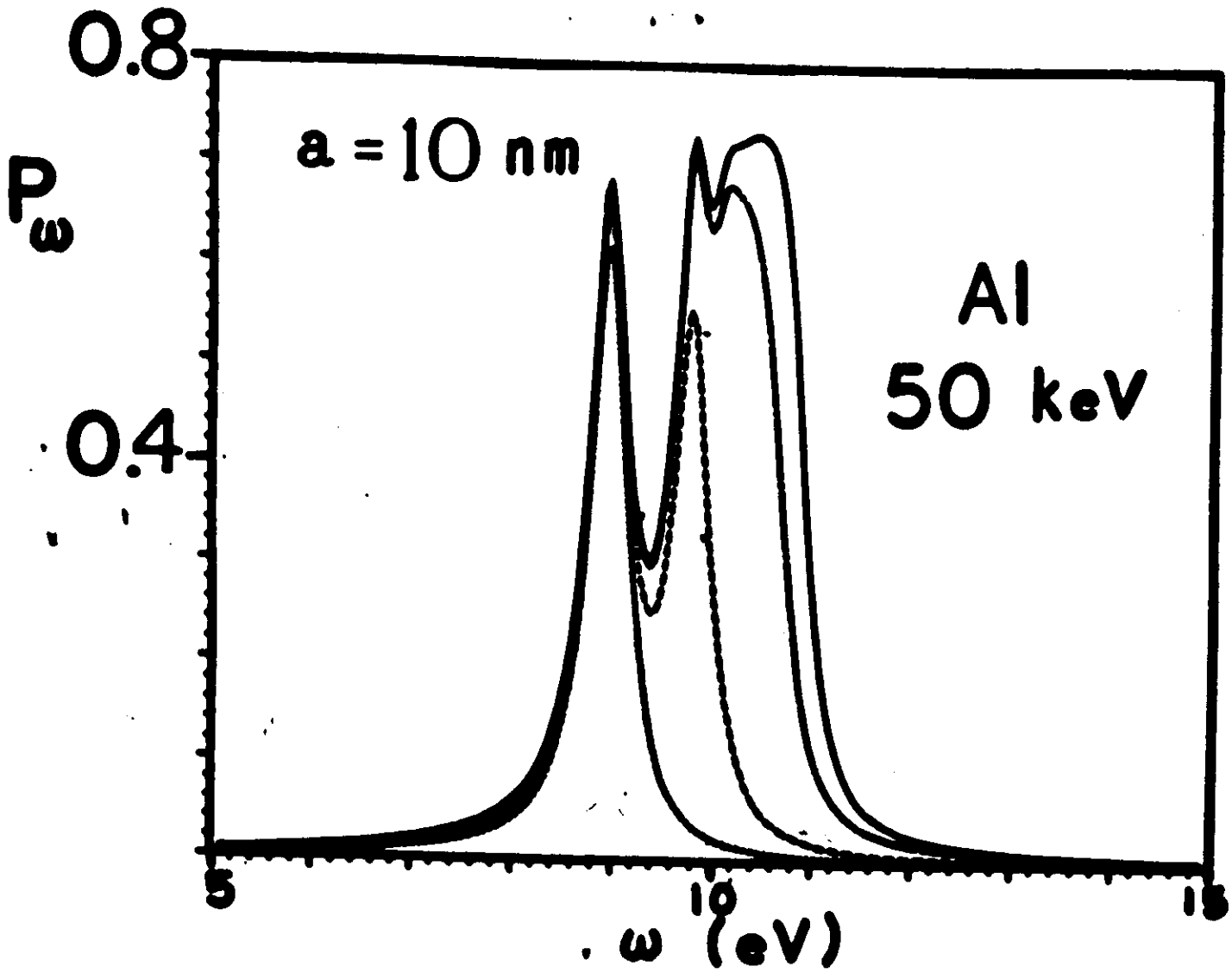
0.8
0.4
P_ω
a = 10 nm
Al
50 keV
5
10
15
ω (eV)

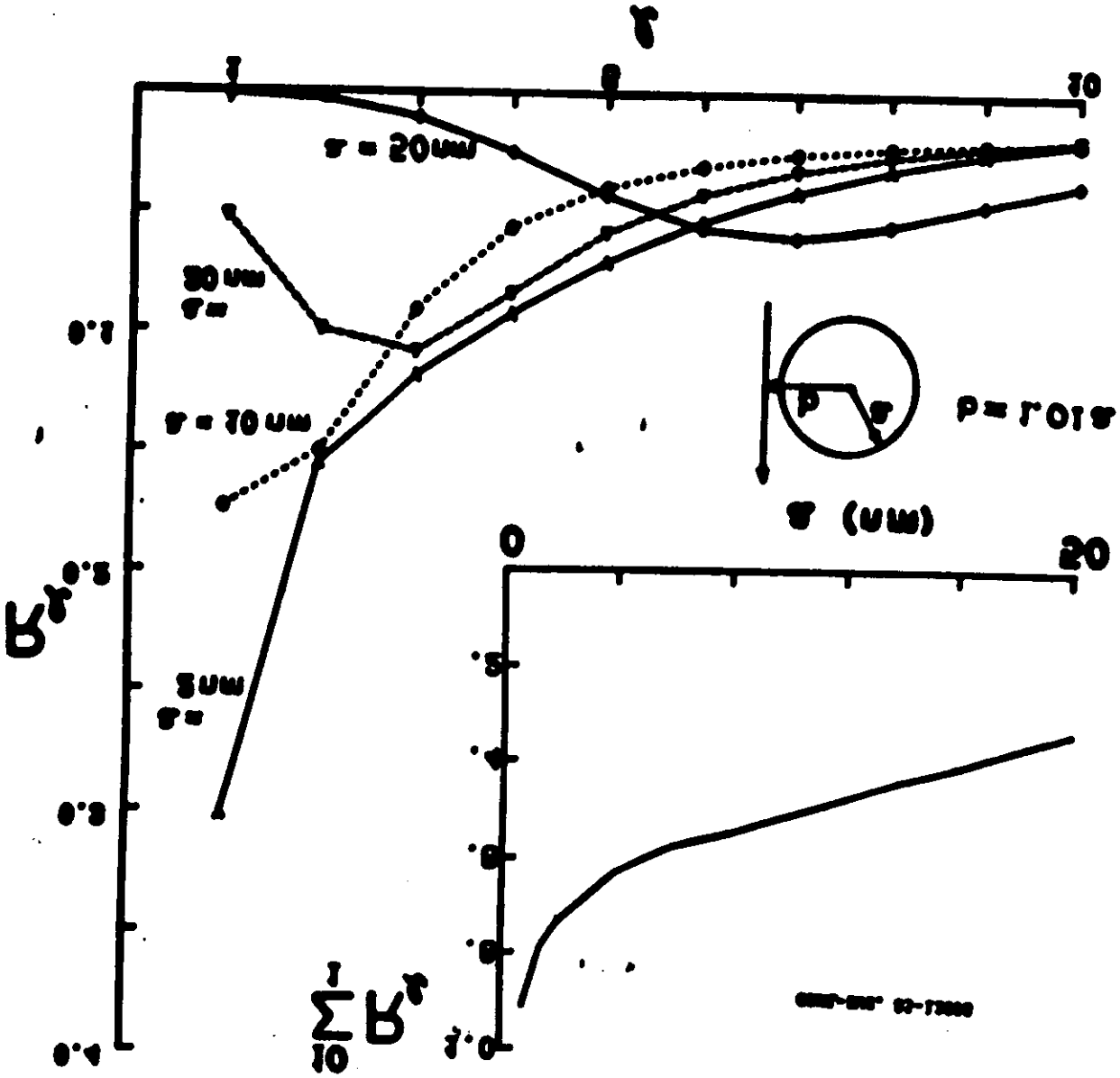
r
1
5
10
r = 20 um
30 um
r =
r = 70 um
5 um
r =
0·1
0·2
0·3
0·4
p = r·01 r
r (um)
0
20
·5
·4
·3
·2
·1
0·0

Ugarte
Phys. Rev. B15

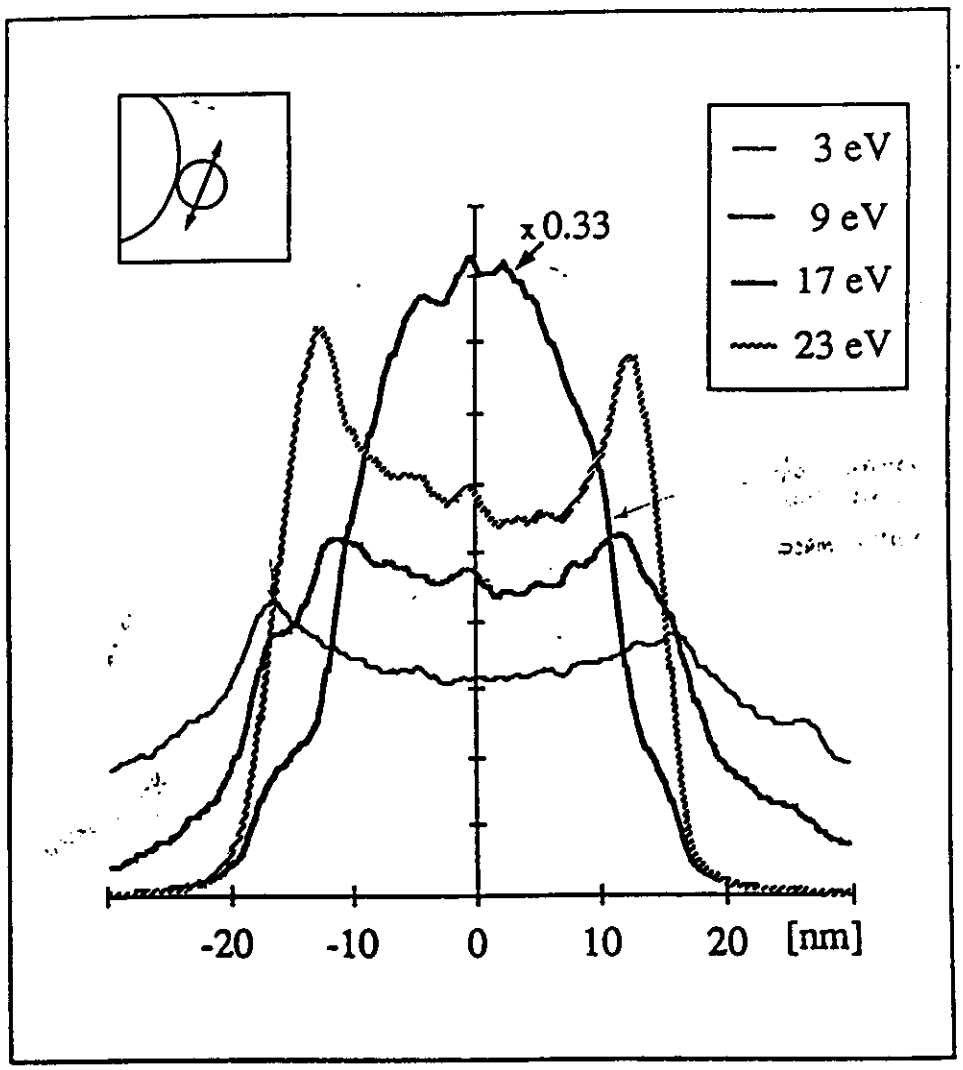

Figure 4

Ugarte, Colloci, Trebbia, Phys Rev B45, 4332 (1992)

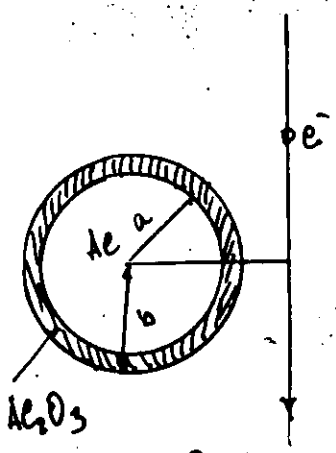

a ~ 50 nm
b ~ 60 nm.

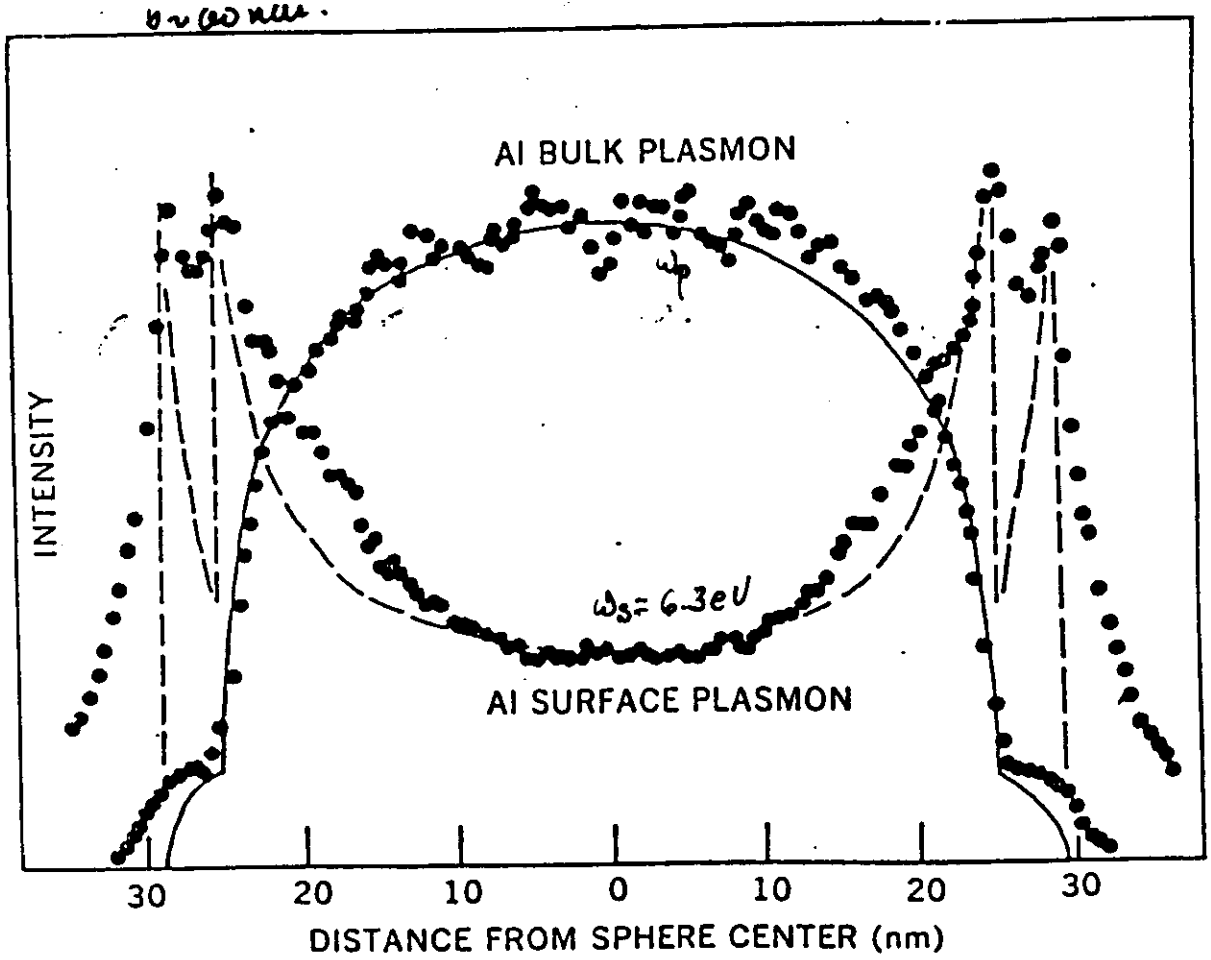

P.E. BATSON and M.M.J. TREACY.

Proc 38th EMSA Meeting S. Francisco CA 1980.

Fig. 5

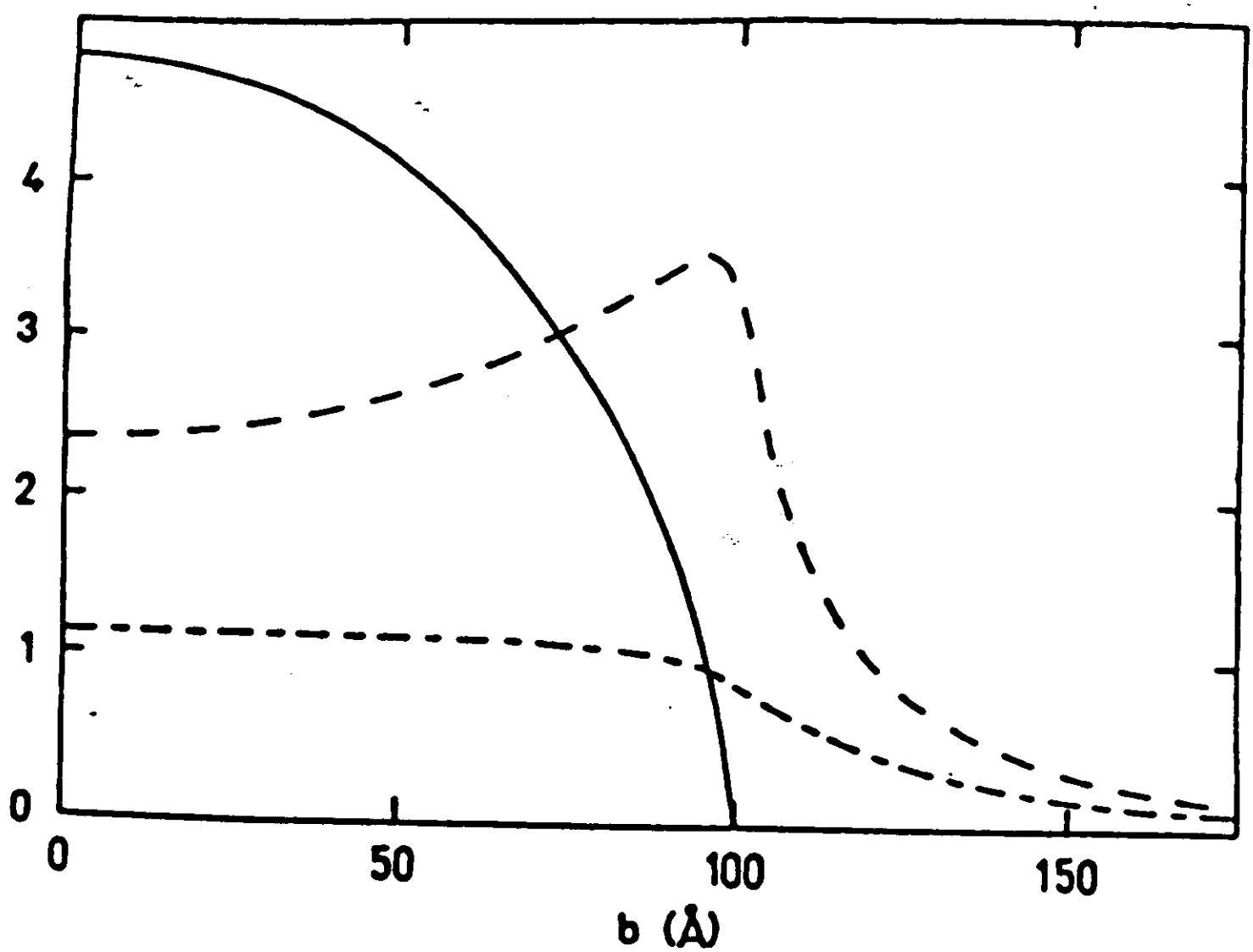

3. Energy-loss probability for a 50 keV electron beam incide
pon an Al sphere of radius 100 Å as a function of the impact par
eter b. Solid line: bulk mode; dashed line: total contribution
he l≤20 surface modes (×6); dashed-dotted line: dipole (l=1) surf
e mode (×6).

Fig. 5

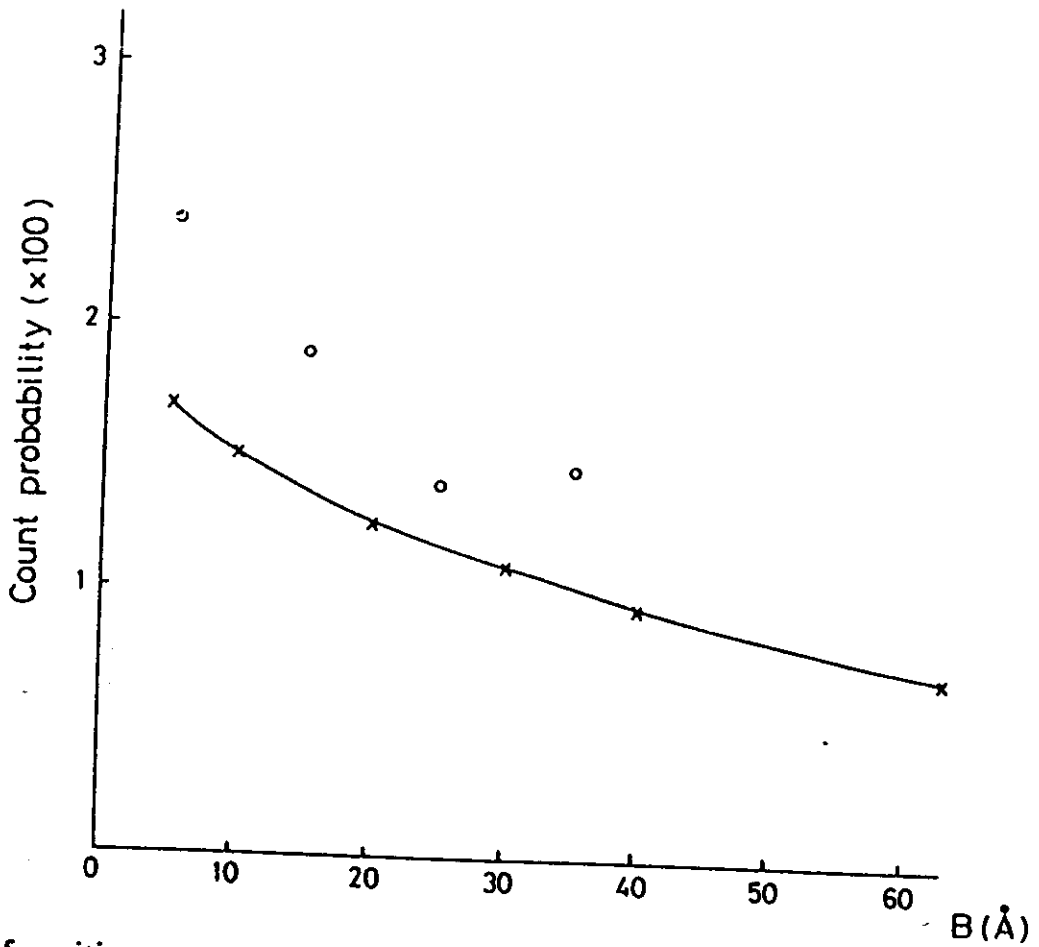

Probability of exciting energy $\hbar\omega$ (over the range 2·3–4·9 eV) as a function of the reduced impact parameter $B = b - a$ for an 80 keV electron incident on an Ag sphere of radius 450 Å: ×, calculation; ○, experimental points.

Fig. 8

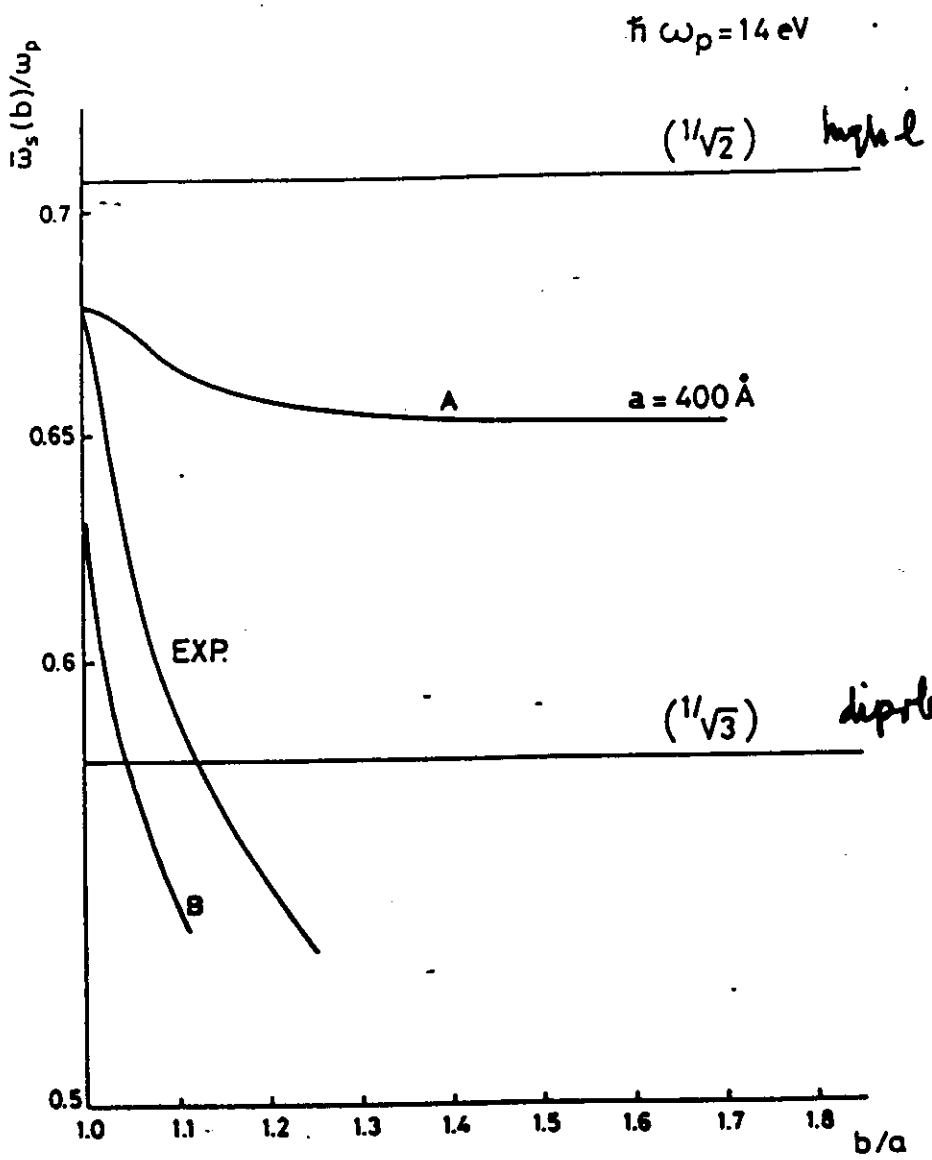

$\omega_s(b) = \frac{\sum_\ell \omega_\ell P^\ell}{\sum P}$

Mean energy loss to surface modes in an Sn particle of radius 400 Å as a function of the impact parameter b: curve A, theoretical curve for zero damping; curve B, includes more realistic damping. (4 eV).

$$P^\ell(b) = \frac{2a}{\pi v^2} \sum_m \frac{2 - \delta_{0m}}{(\ell-m)!(\ell+m)!} \omega_\ell \left(\frac{\omega_\ell a}{v}\right)^{2\ell} K_m^2\left(\frac{\omega_\ell b}{v}\right)$$

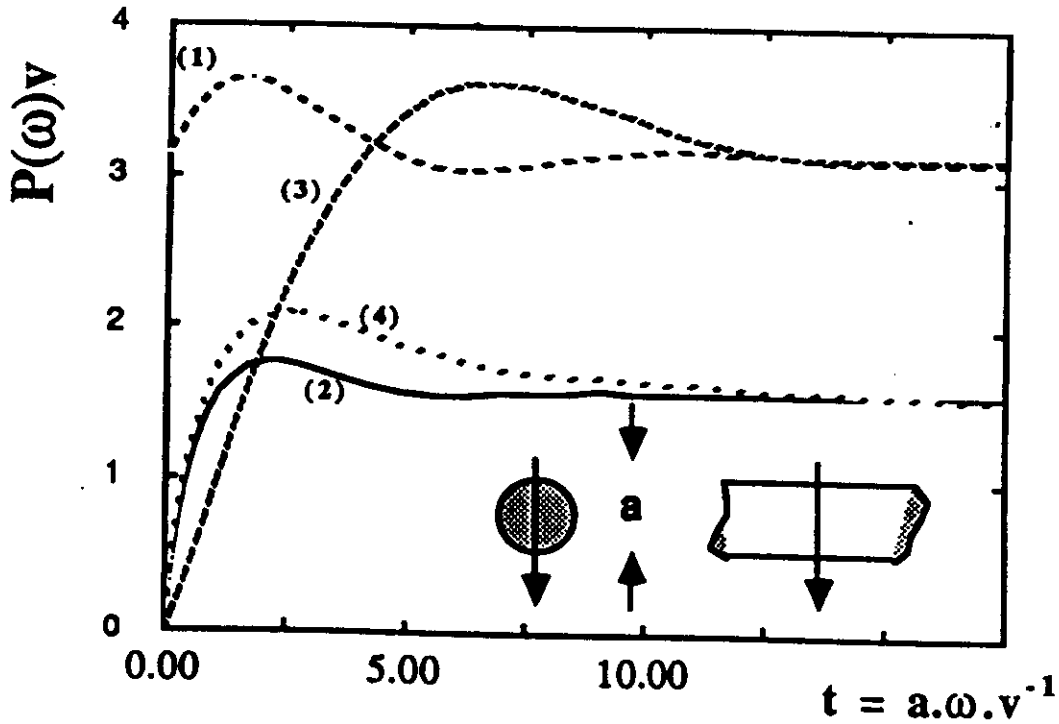
P(ω)v
4
3
2
1
0
(1)
(3)
(4)
(2)
a
0.00
5.00
10.00
t = a.ω.v^-1

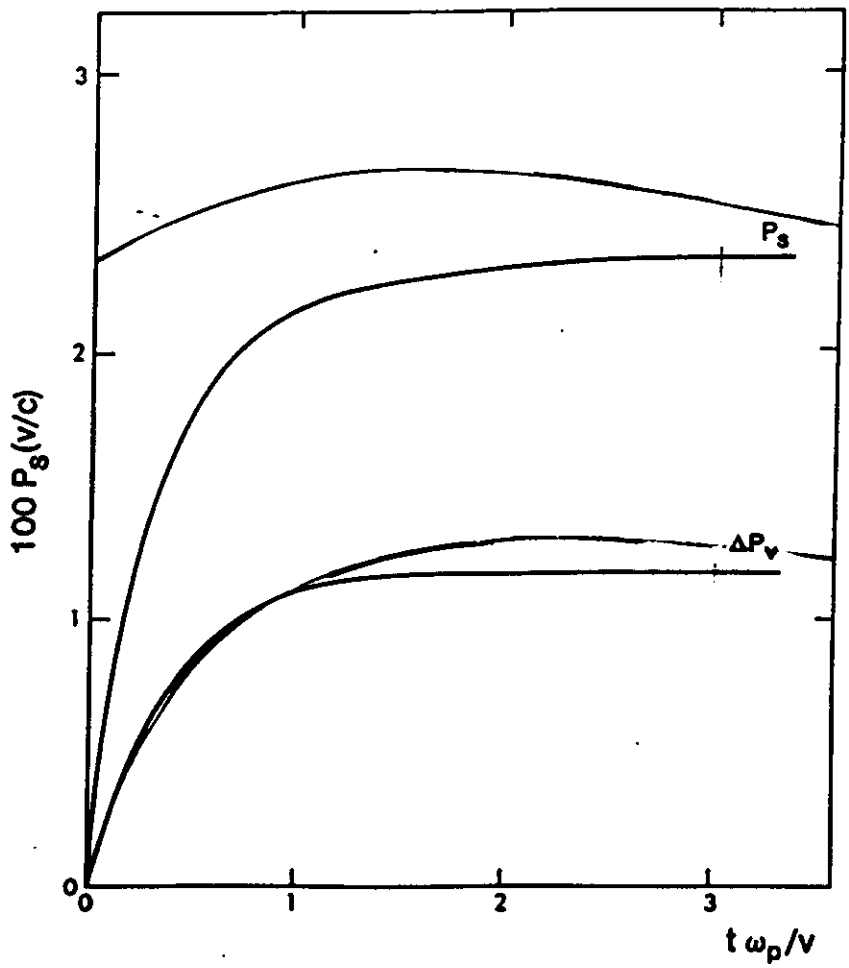

Figure 3.24. Total probability P_s of surface-plasmon excitation (by normally incident electrons of velocity v) for a sample with two clean surfaces, calculated as a function of specimen thickness t assuming a free-electron model (Ritchie, 1957). Also shown is the reduction ΔP_s in the probability of volume-plasmon excitation.

Surface $P = P_+ + P_-$

$\omega = \omega_s (\alpha_\pm)^{1/2}$

$\alpha_\pm = 1 \pm e^{-Qa}$

$a \to 0$ $P_+ \propto a \to 0$

$P_- \to \pi/v$!

$\omega_- P_- \to \sqrt{a} \to 0$

Probability of excitating surface plasmons in films

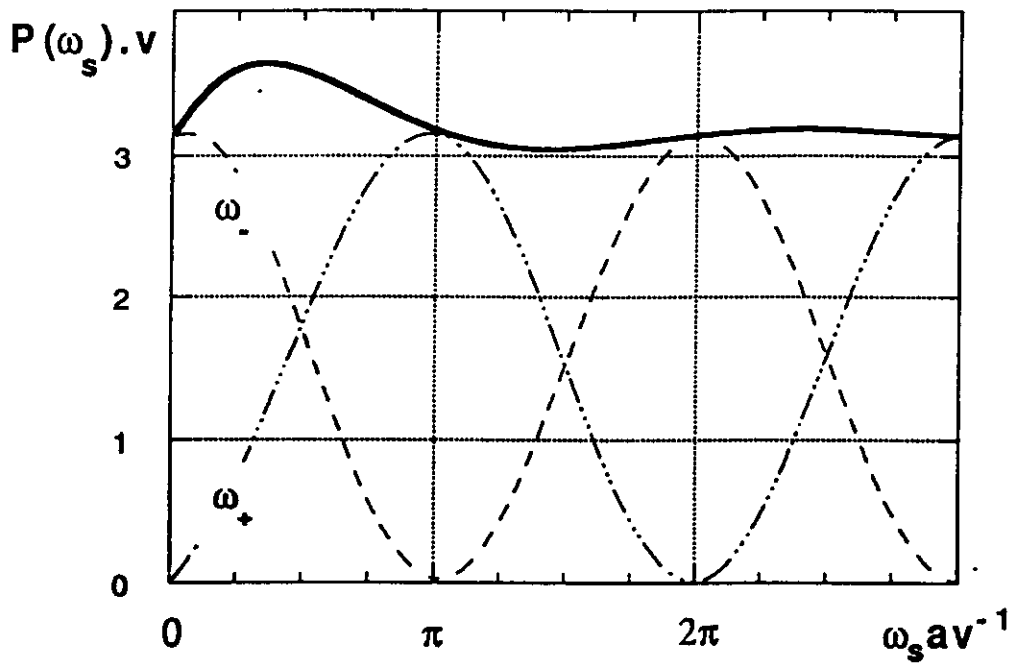

Surface energy loss in films

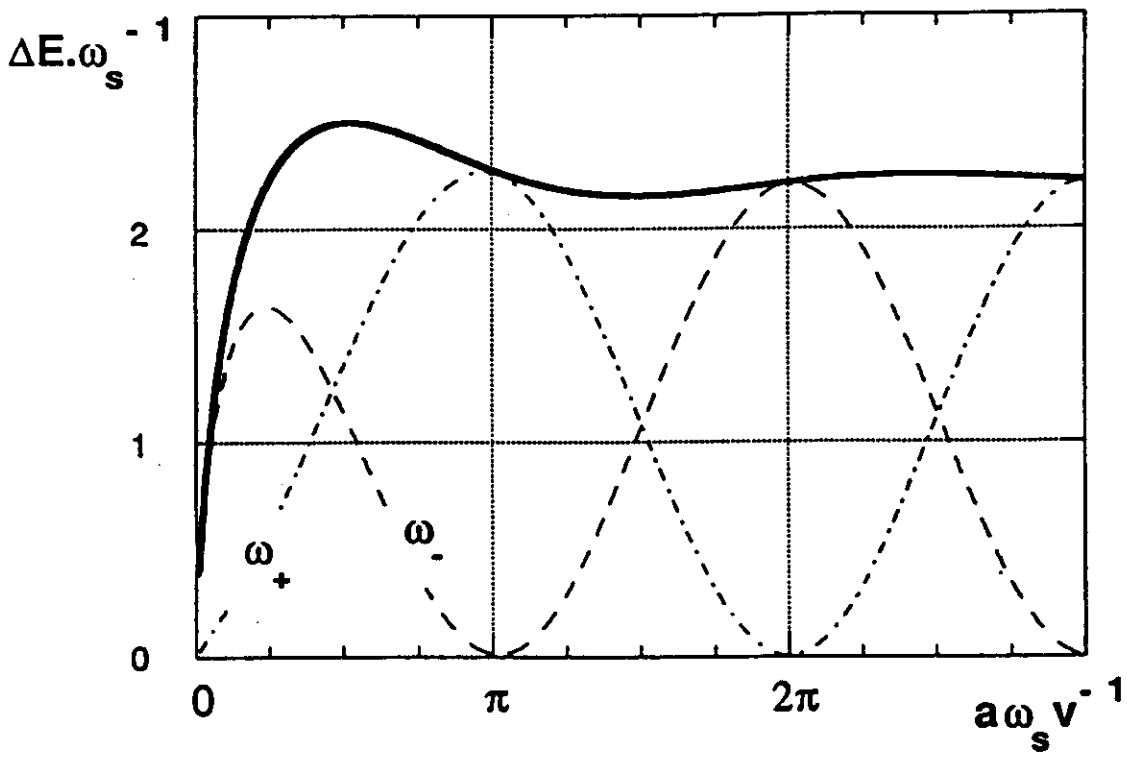

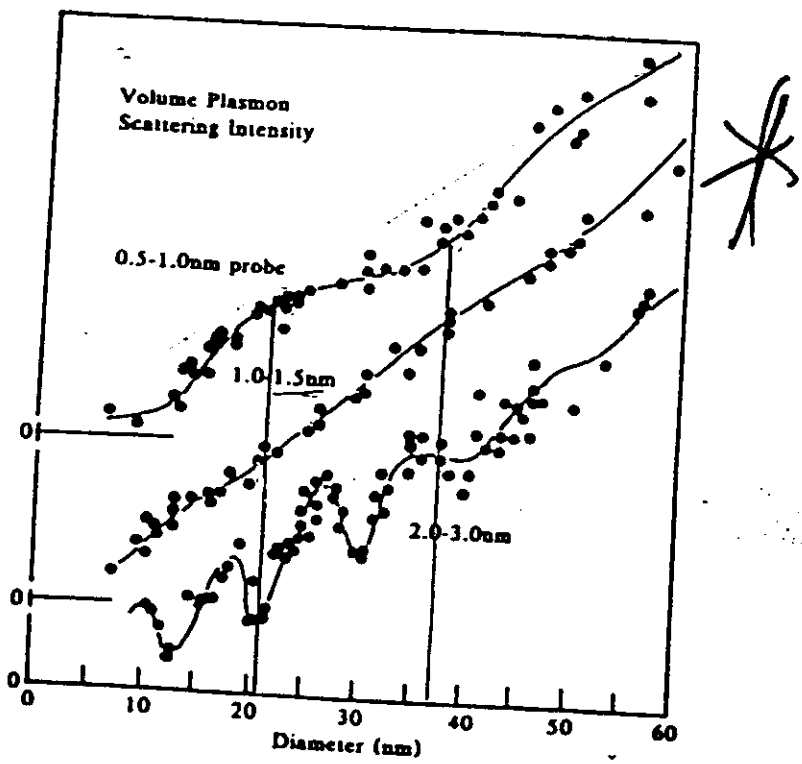

Figure 5. Scattering probability for bulk plasmons in small spheres as a function of sphere diameter, for three different probe conditions. The deep oscillations are due to interference between the probe spatial frequencies and spatial quantization of the bulk plasmon within the sphere.

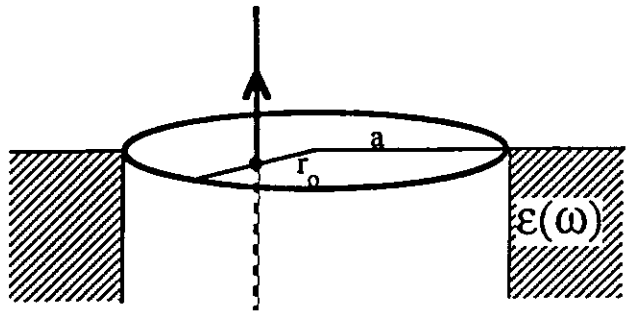

$$P_{r_o}(\omega) = \frac{2}{\pi V^2} \sum_{m=0} (2 - \delta_{om})\, I_m^2(R_o)\, \mathrm{Im}\left[\frac{K_m(A)\, K'_m(A)\, (\varepsilon-1)}{X_m}\right] \qquad r_o < a$$

$$P_{r_o}(\omega) = \frac{2}{\pi V^2} \sum_{m=0} (2 - \delta_{om})\, K_m^2(R_o)\, \mathrm{Im}\left[\frac{I_m(A)\, I'_m(A)\, (\varepsilon-1)}{\varepsilon X_m}\right]$$

$$X_m = I_m(A)\, K'_m(A)\, \varepsilon - I'_m(A)\, K_m(A)$$

$$R_o = \frac{\omega r_o}{v} \qquad A = \frac{\omega a}{v}$$

<u>Relativistic</u> Axial $r_o = 0$

$$P_\infty(\omega) = \frac{2}{\pi V^2 \gamma^2}\, \mathrm{Im}\left[\frac{\varepsilon \nu_o K_o(\nu_o a)\, K_1(\nu a) - \nu K_o(\nu a)\, K_1(\nu_o a)}{\varepsilon \nu_o K_1(\nu a)\, I_o(\nu_o a) + \nu K_o(\nu a)\, I_1(\nu_o a)}\right]$$

$$\gamma = 1/\sqrt{1-\beta^2}\,; \qquad \beta = \frac{v}{c}$$

$$\nu_o = \frac{\omega}{v}\sqrt{1 - \beta^2} = \frac{\omega}{v\gamma}\,; \qquad \nu = \frac{\omega}{v}\sqrt{1 - \varepsilon\beta^2}$$

Effective dielectric response theory

1) Simple averaging $(\varepsilon_{eff} = \bar{\varepsilon} = f\,\varepsilon_A + (1-f)\,\varepsilon_B)$

2) Maxwell-Garnett $\varepsilon_{eff} = \varepsilon_B \dfrac{\left((1+2f)\,\varepsilon_A + 2\,(1-f)\,\varepsilon_B\right)}{\left((1-f)\,\varepsilon_A + (2+f)\,\varepsilon_B\right)}$

3) Bruggeman $f\dfrac{\varepsilon_{eff} - \varepsilon_A}{2\,\varepsilon_{eff} + \varepsilon_A} + (1-f)\dfrac{\varepsilon_{eff} - \varepsilon_B}{2\,\varepsilon_{eff} + \varepsilon_B} = 0$

4) Mixture of closely similar dielectric $\varepsilon_{eff} = \bar{\varepsilon} - f(f-1)(\varepsilon_A - \varepsilon_B)^2 / 3\bar{\varepsilon}$
(Landau and Lifshitz)

Excitation theory based on electron trajectories

$$\mathrm{Im}\left(\frac{-1}{e_{eff}}\right) = \begin{array}{l} f\left(\mathrm{Im}\left(\frac{-1}{e_A}\right) + g_{INT}\left(\mathrm{Im}\left(\frac{-3}{e_A + 2\,\varepsilon_B}\right) - \mathrm{Im}\left(\frac{-1}{e_A}\right)\right)\right) \\ +(1-f)\left(\mathrm{Im}\left(\frac{-1}{e_B}\right) + g_{ext}\left(\mathrm{Im}\left(\frac{-3}{e_A + 2\,\varepsilon_B}\right) - \mathrm{Im}\left(\frac{-1}{e_B}\right)\right)\right) \end{array}$$

$g_{int} \rightarrow$ } relative importance of interface to bulk excitations in the small spheres of material A

g_{ext}

$$g_{int} = \frac{1}{1 + \frac{3\,a\omega}{\upsilon}};$$

This leads for $g_{int} = 1$ and to for $g_{ext} = 2f/1+2f$ (seems reasonable) to the Maxwell-Garnett expression: which can be rewritten in the form

$$\mathrm{Im}\left(\frac{-1}{\varepsilon_{eff}}\right) = \mathrm{Im}\left(\frac{-1}{\varepsilon_B}\right) + \frac{3f}{1+2f}\left(\mathrm{Im}\left(-\frac{3}{(1+2f)\,\varepsilon_A + 2(1-f)\,\varepsilon_B}\right) - \mathrm{Im}\left(-\frac{1}{\varepsilon_B}\right)\right)$$

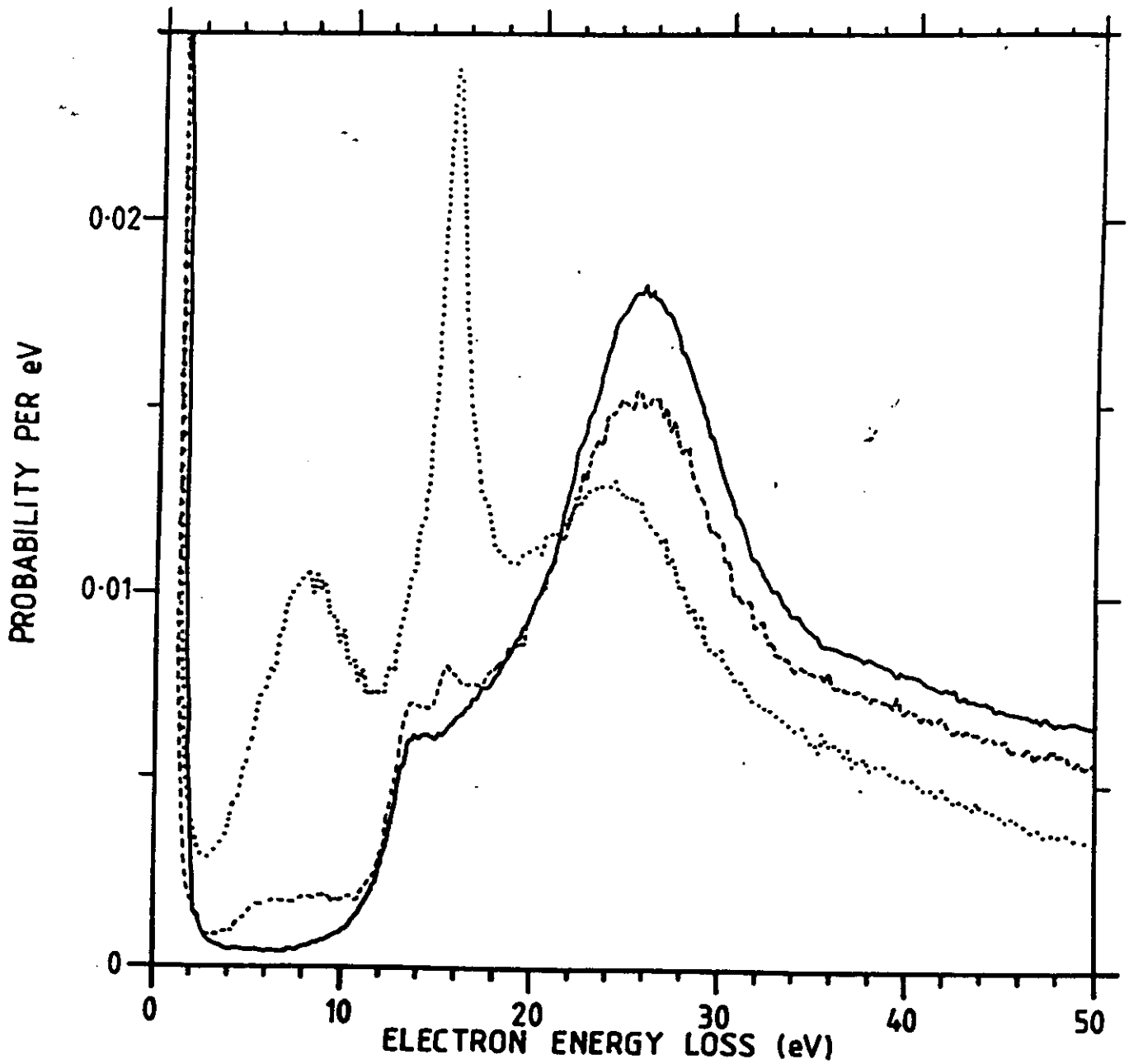
0·02
0·01
0
PROBABILITY PER eV
0
10
20
30
40
50
ELECTRON ENERGY LOSS (eV)

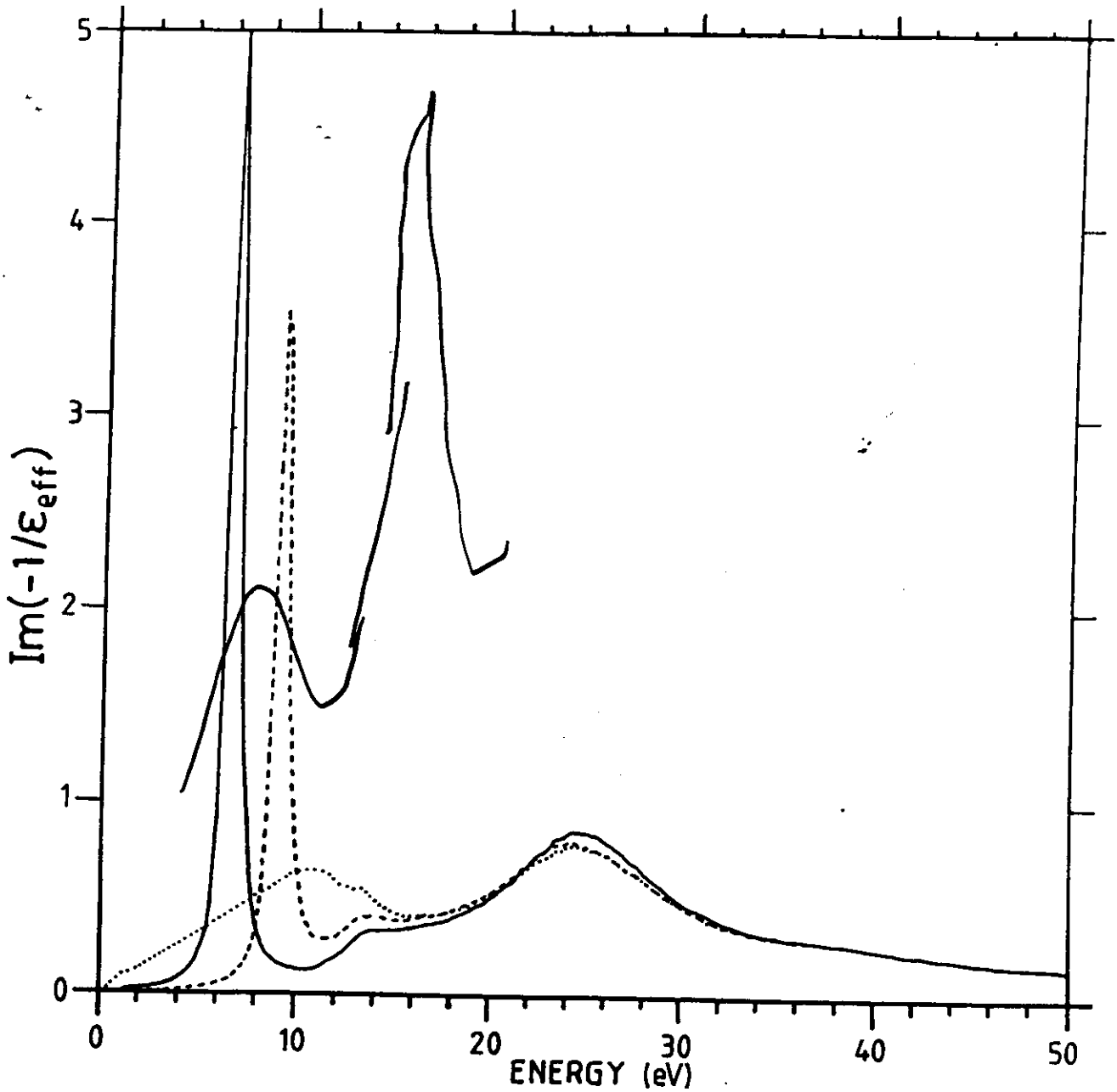
5
4
3
2
1
0
0
10
20
30
40
50
ENERGY (eV)
Im(-1/ε_eff)

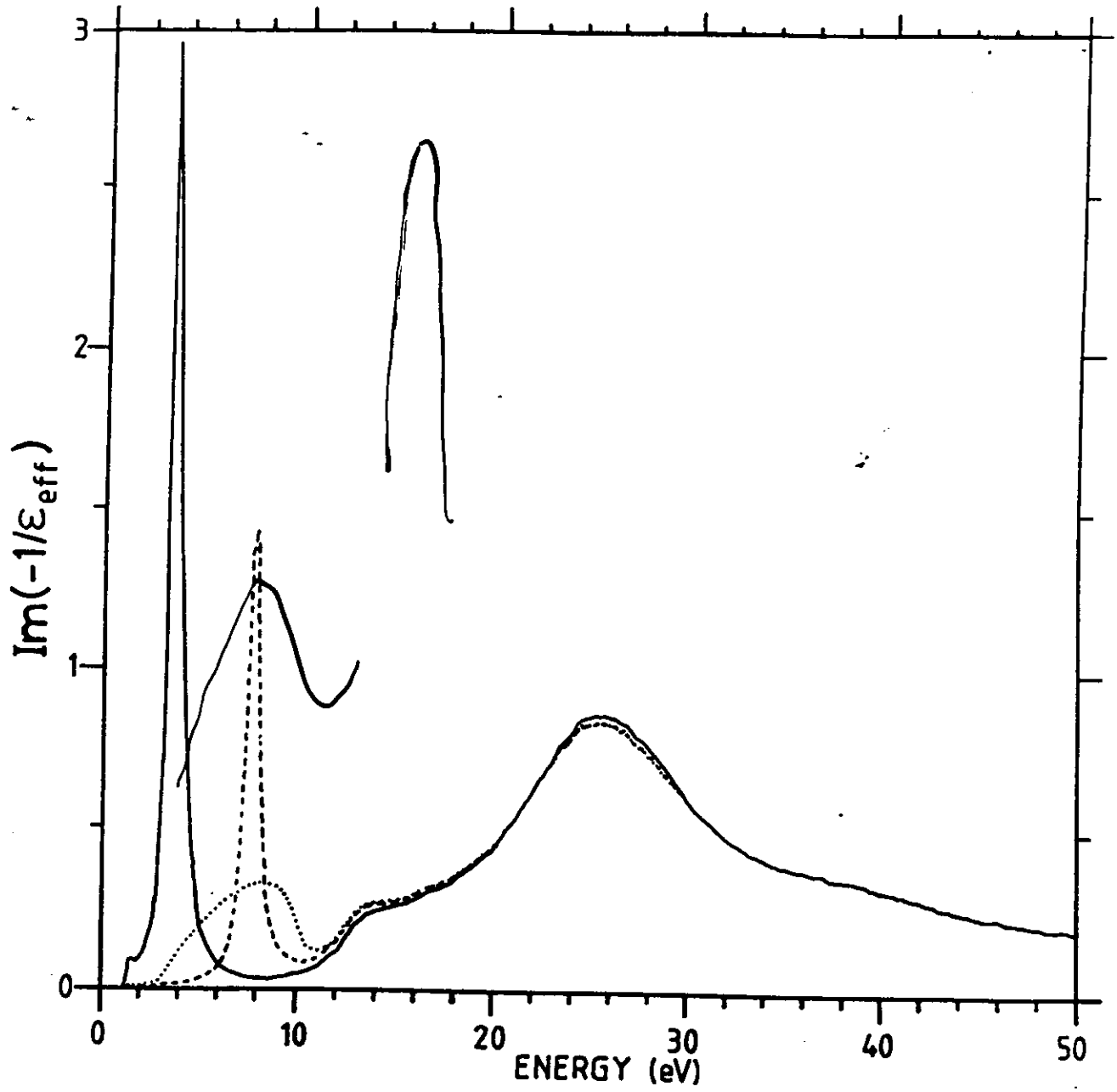
3
2
1
0
$Im(-1/\varepsilon_{eff})$
0
10
20
30
40
50
ENERGY (eV)

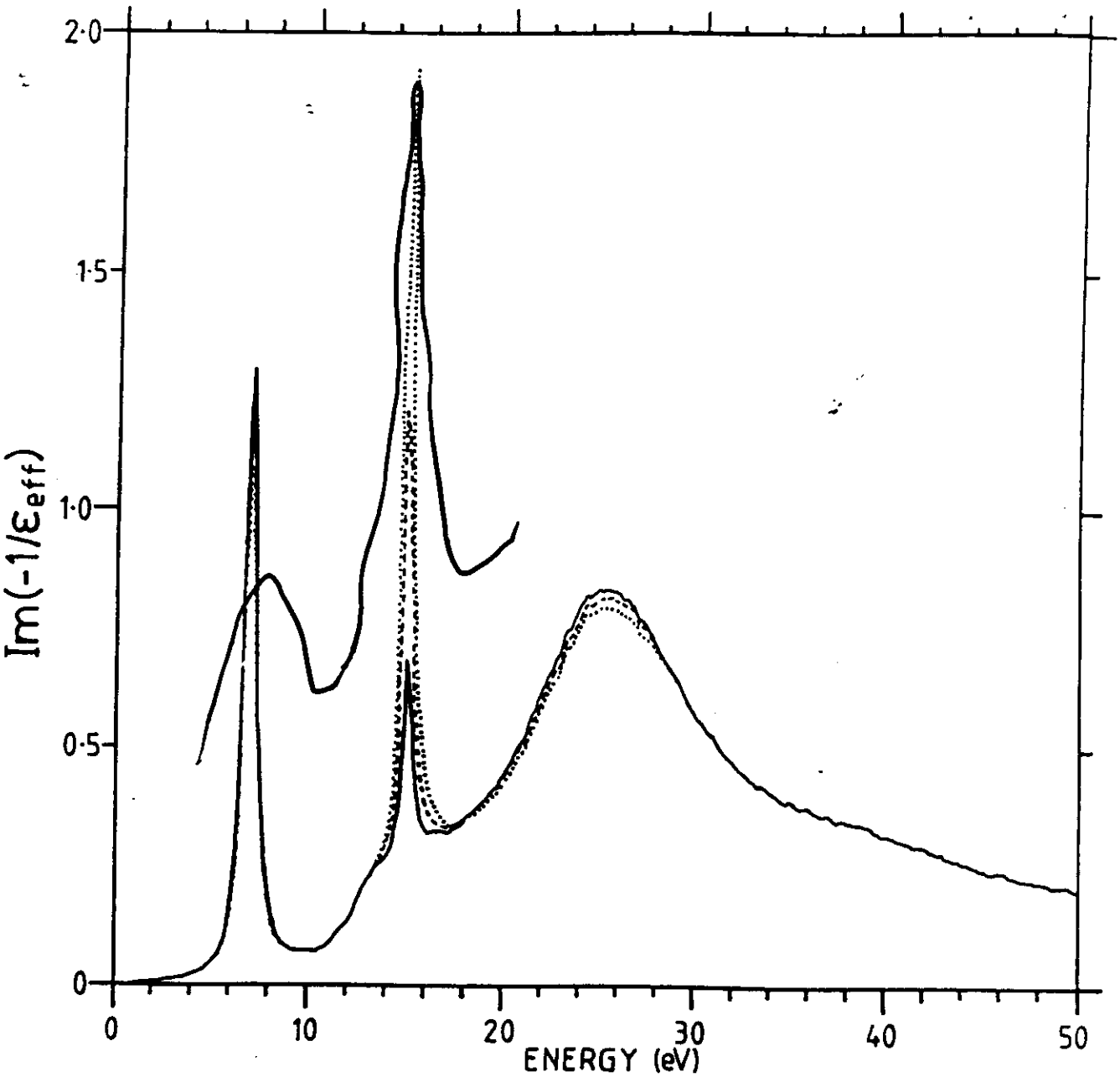
2·0
1·5
1·0
0·5
0
Im(-1/ε_eff)
0
10
20
30
40
50
ENERGY (eV)

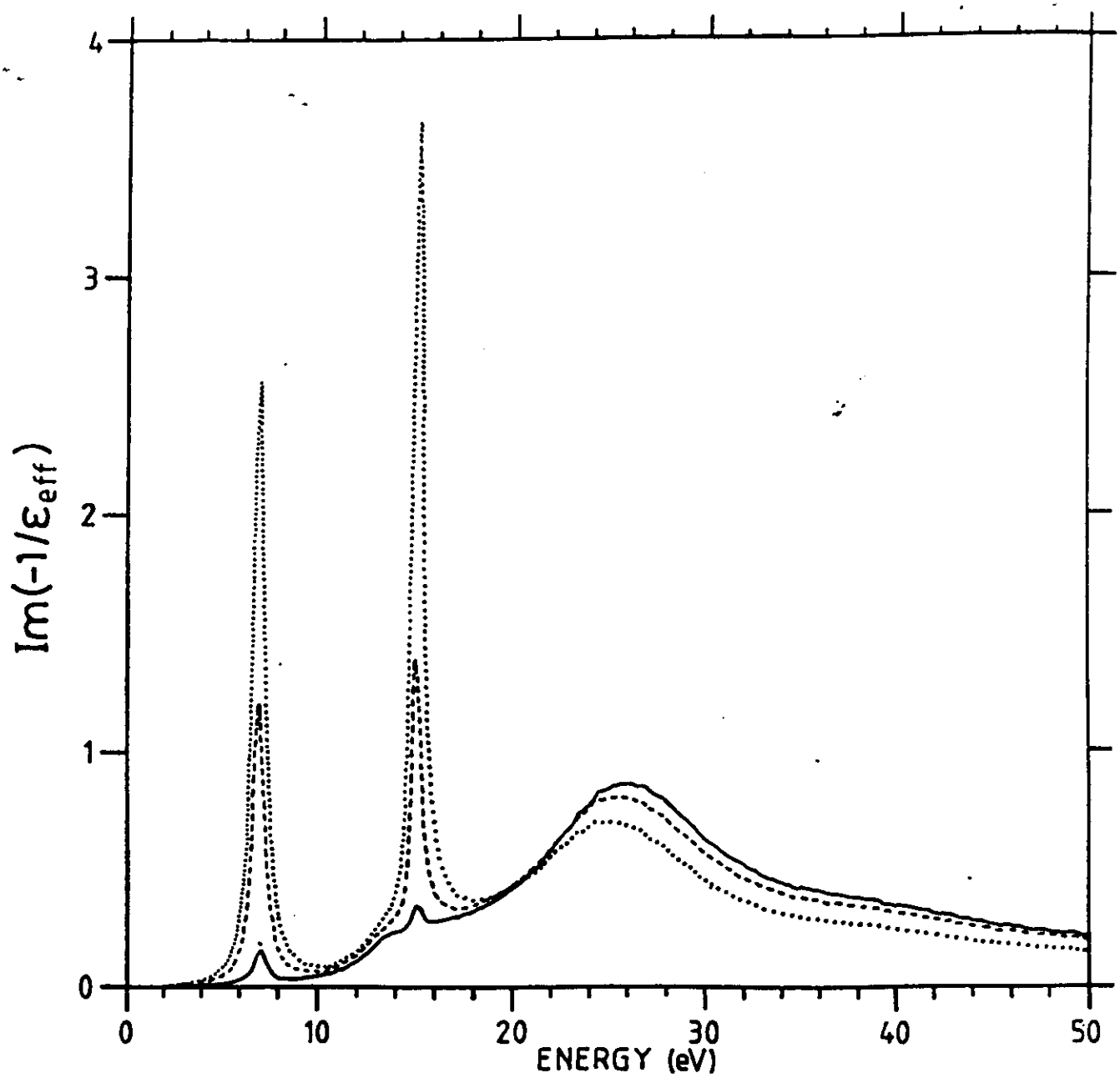
4
3
2
1
0
Im(-1/ε_eff)
0
10
20
30
40
50
ENERGY (eV)

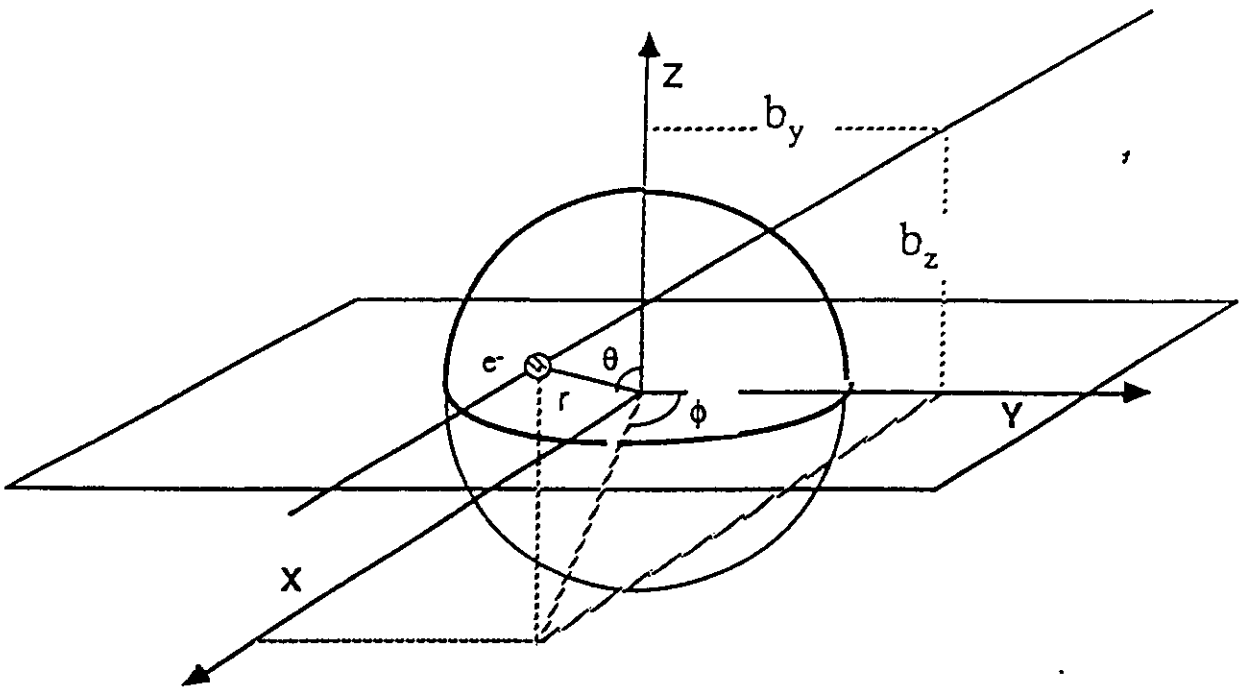

Fig I

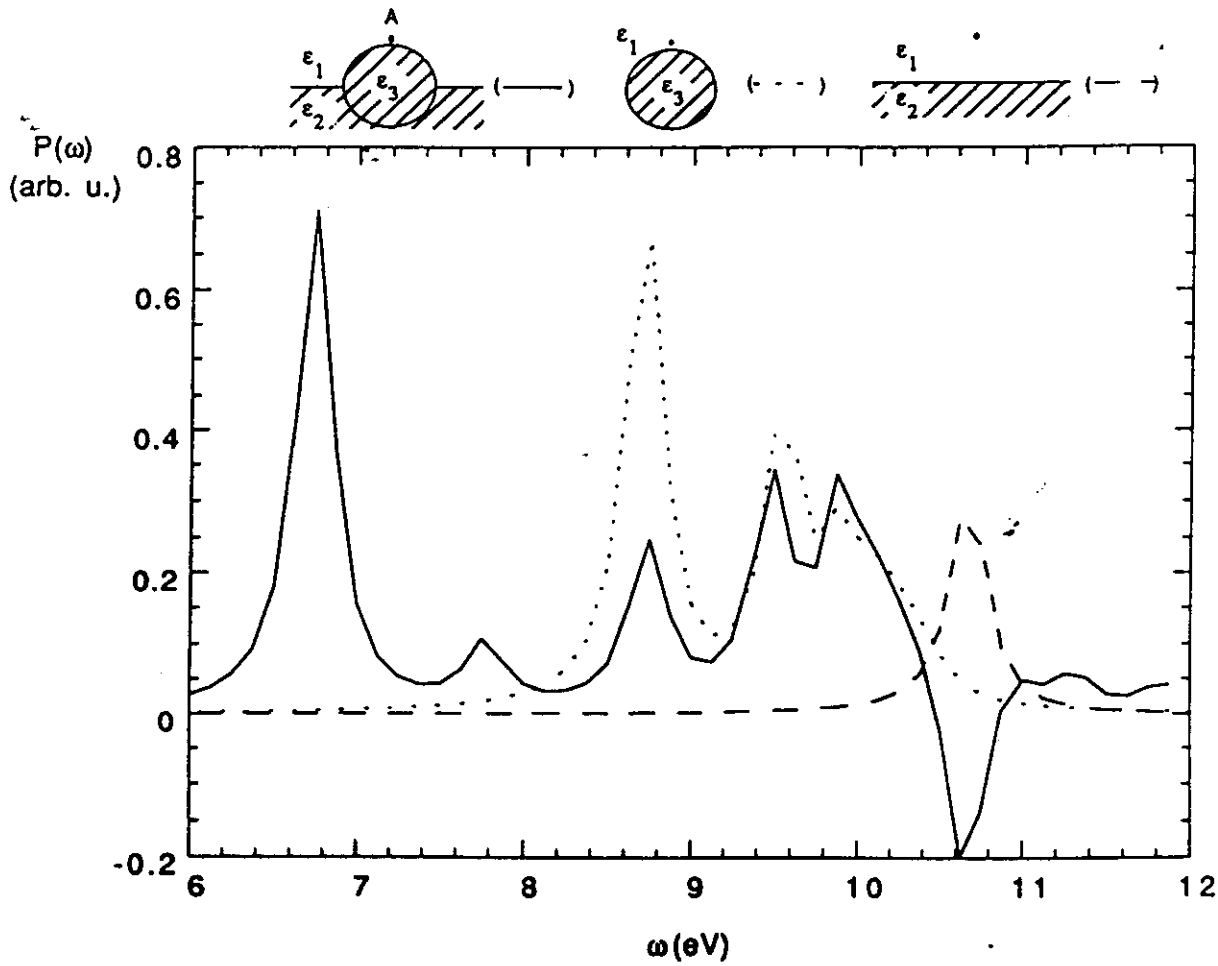
A
ε1
ε3
ε2
ε1
ε3
ε1
ε2
P(ω)
(arb. u.)
0.8
0.6
0.4
0.2
0
-0.2
6
7
8
9
10
11
12
ω(eV)

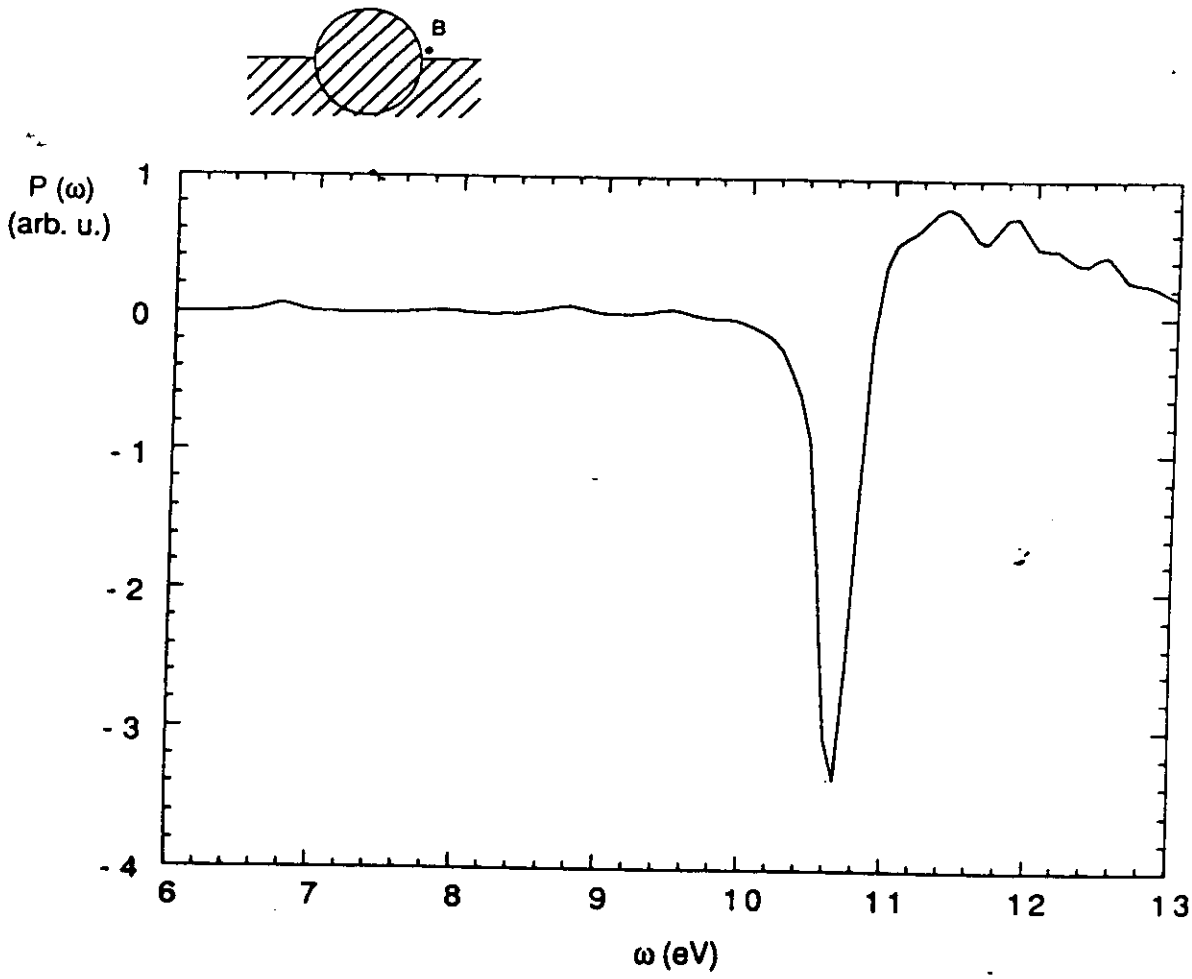

Fig. ...

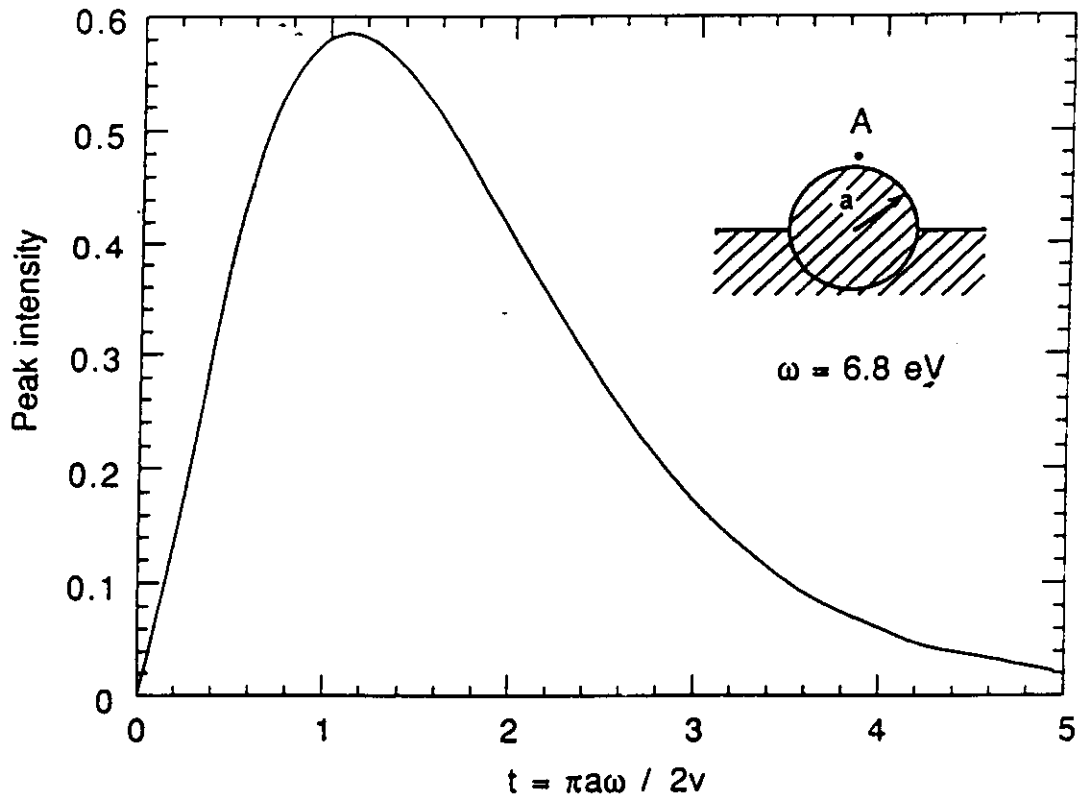

FIG 3

SECONDARY ELECTRON GENERATION PROCESS AND THEIR DEGREE OF LOCALIZATION.

STEM Recent work by Howie et al (1985,1989) has shown that it is possible to obtain SE signals with 1nm spatial resolution and 1eV energy resolution (and that reflection SE images of oxidized Cu show oxide islands and their interaction with surface steps)

Generation of SE.

Complex process
- Electron cascade process
- Slowing down - knockons
- Decay of inner shells
- Decay of collectives states

Chung and Everhart
Rosler, Braner
Luo and Joy

Localization

Relevant impact parameter or distance from the electron beam where the secondary e^- is generated.

Energy transfer method. (Ritchie et al (1990))

DIMPFT → Impact Parameter

$$\frac{d^2\Lambda^{-1}_{ET}}{d^2b} = \frac{1}{\pi^2 v^3}\int_0^{\infty}\omega\, d\omega \int_0^{\infty}\frac{\kappa\, d\kappa}{k^2}\left[\frac{\omega}{v}K_0\left[\frac{\omega b}{v}\right]J_0(\kappa b) + \kappa K_1(\kappa b)\, J_1\left[\frac{\omega b}{v}\right]\right] \mathrm{Im}\left[\frac{-1}{\varepsilon_{k,\omega}}\right]$$

It appears that the narrow spatial resolution of these IPR distributions is due to the presence of relatively large momentum components in the interaccion spectruim of the swift electron and the electron gas.

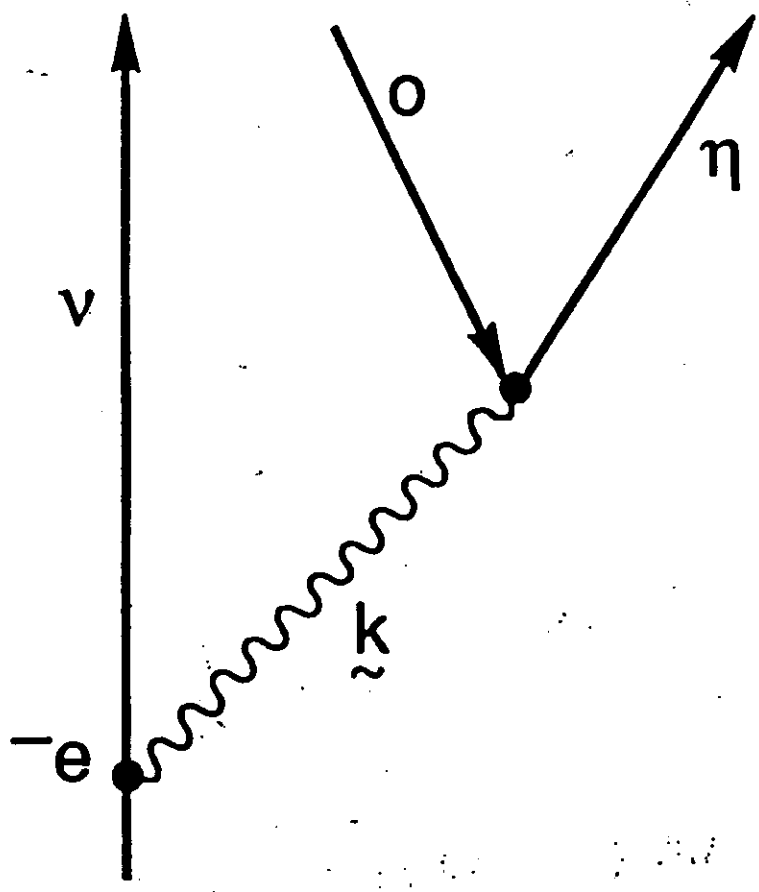

Figure 5. A Feynman diagram representing the process of creation of a virtual quasi-particle followed by the excitation of an electron-hole pair in the medium.

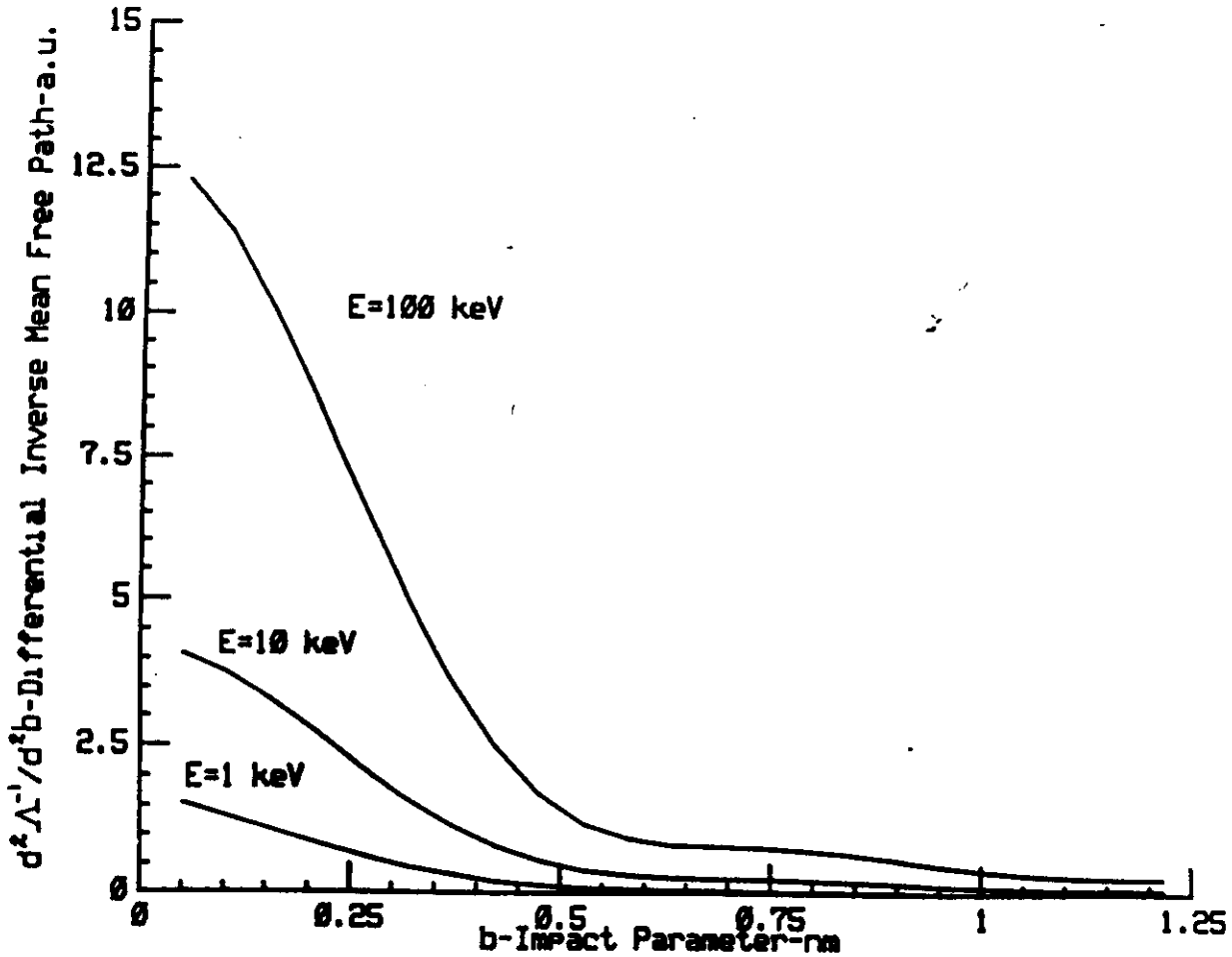

Figure 6. A plot of $d^2\Lambda^{-1}/d^2b$, the inverse mean free path differential in impact parameter b, versus b, for three different electron energies, calculated from Eq. 28. For convenience in plotting, the curves have been scaled by multiplying the results from Eq. 28 by the factor $2\pi\hbar v^3/e^2\omega_p^2$, where v is the electron speed.

Millegans, Howie, Tomita, Bleloch.
Cavendish Lab — Cambridge (1992)

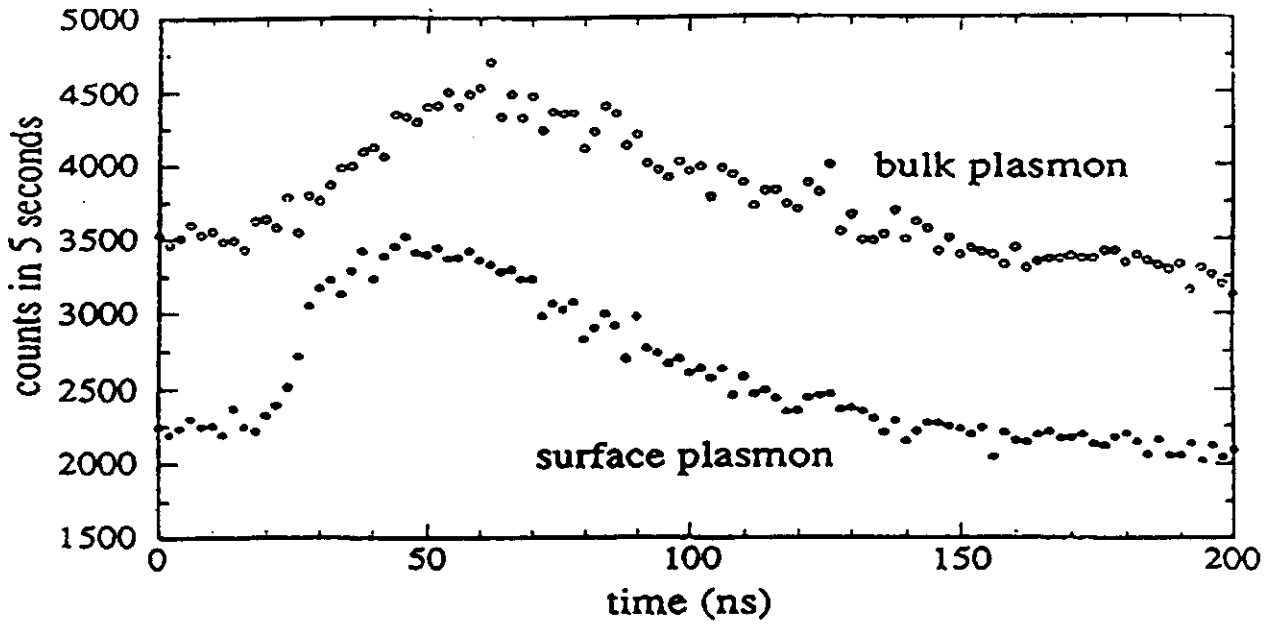

Fig. 1. Time-spectra for primary energy loss corresponding to surface (21 eV) and bulk plasmon energy (34 eV) in CVD diamond.

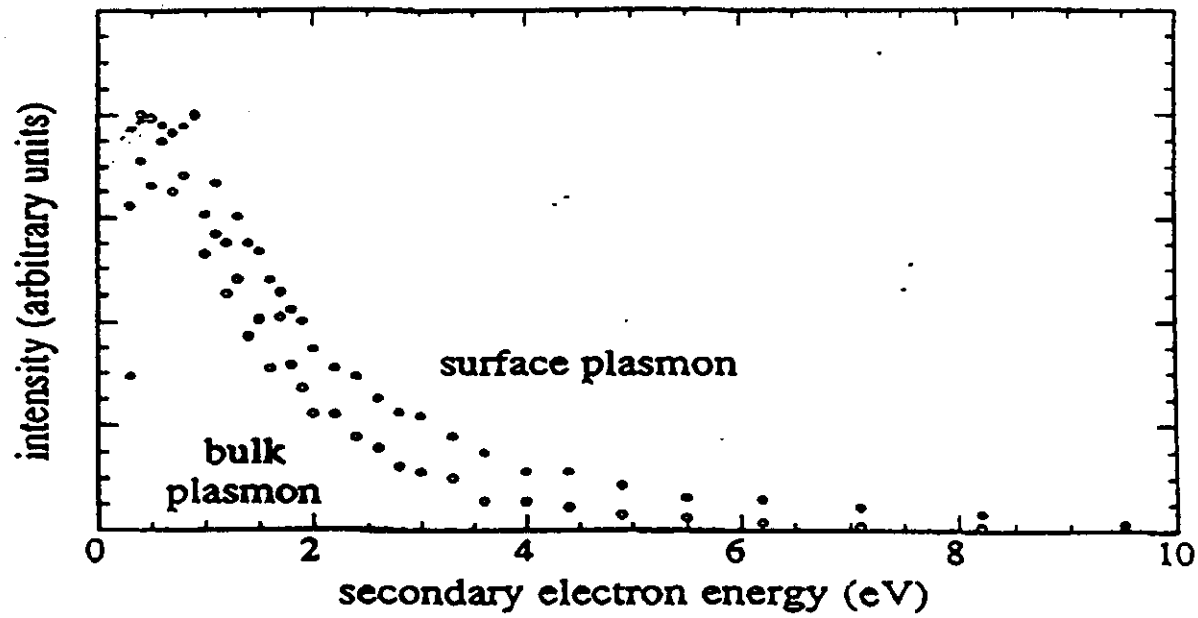

Fig. 2. Secondary electron spectra generated by surface and bulk plasmon energy loss in CVD diamond calculated from the time-spectra in figure 1. The spectra are normalized to the same maximum number of counts.

Pilper & P. Kruit – Phys Rev B 44, 17 (1991)

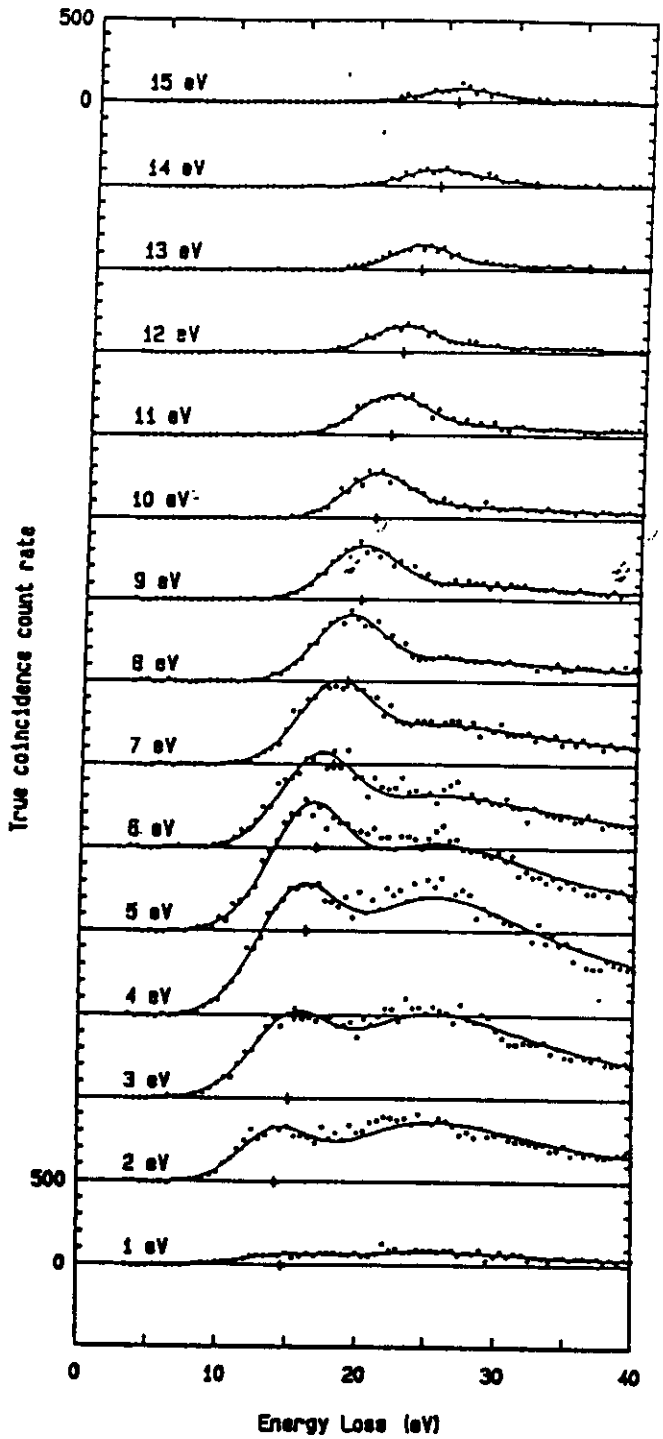

DEFLECTING FORCE

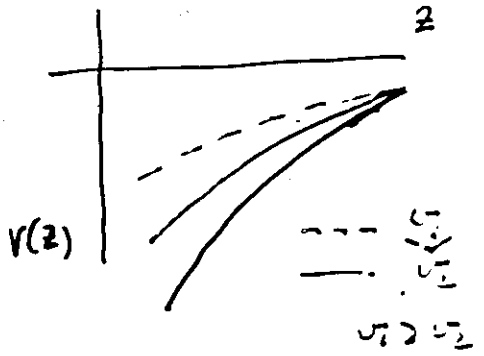

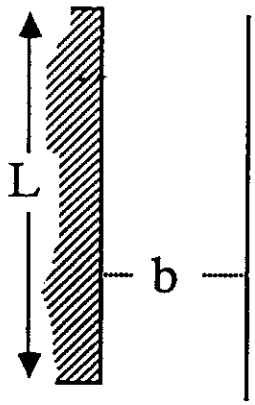

$$\Delta\theta \sim \frac{F_\perp t}{V} \sim \frac{(\omega_s/V)^2 (L/V)}{V} = \frac{L\,\omega_s^2}{V^4} \sim 10^{-6} \text{ rads.}$$

3 orders of magnitude ~~greater~~ smaller than experiment (Cowley!).

E. A. Howie → $\sim 10^{-6}$ rads

$\Delta\theta$ ~ infinite medium but L!

SPHERE

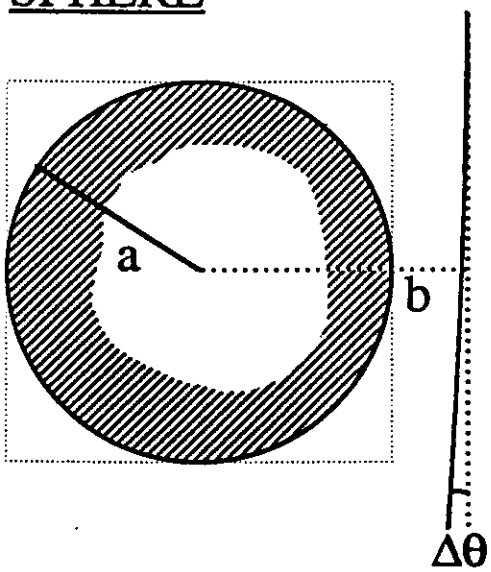

$$\Delta\theta = \frac{4}{\pi V^3} \sum_{l\,m} \frac{2 - \delta_{om}}{(l-m)!(l+m)!} \int_0^\infty R_e[\gamma_l(\omega)] \left(\frac{\omega a}{V}\right)^{2l+1} K_m\left(\frac{\omega b}{V}\right) K'_m\left(\frac{\omega b}{V}\right) d\omega$$

when $K'_m(x)$ indicates derivative with respect to x

DEFLECTION OF ELECTRONS BY AL SPHERES.

Dependence of θ with B=b-a (at constant a)

Free electron ε(ω) with damping

E_e=100Kev